

Supporting Information

for

Acid-base catalysis in the mechanochemical formation of a reluctant imine

by

Leonarda Vugrin, Ivica Cvrtila, Marina Juribašić Kulcsár, Ivan Halasz*

Ruđer Bošković Institute, Bijenička c. 54, 10000 Zagreb, Croatia

Email: ivan.halasz@irb.hr

Table of contents

1. General information	1
1.1. Chemicals	1
1.2. Milling equipment	1
1.3. Nuclear Magnetic Resonance (NMR) spectroscopy	1
1.4. Powder X-Ray diffraction (PXRD)	1
1.5. Infrared spectroscopy (IR)	2
1.6. Computational details	2
1.7. Imine synthesis procedure	2
2. Figures	3
2.1. Raman	3
2.2. PXRD	17
2.3. IR	19
2.4. NMR	20
3.0. References	54

1. General information

1.1. Chemicals

4-nitrobenzaldehyde (Alfa Aesar), 4-nitroaniline (Fluka), ammonium acetate (Riedel-de Haën), sulfamic acid (Kemika), acetonitrile (BDH Prolabo), nitromethane (Kemika), dimethylformamide (Gram-mol), acetic acid (T.T.T.), n-heptane (Kemika), diethyl ether (Gram-mol), 2-propanol (T.T.T.), methanol (Lach-Ner), acetone (Lach-Ner), triethylamine (Riedel-de Haën), benzoic acid (Alfa Aesar), citric acid (Kemika), methacrylic acid (Alfa Aesar) and 1,8-diazabicyclo[5.4.0]undec-7-ene (Alfa Aesar) were used as received from commercial suppliers. The starting materials are compounds with high melting points, m.p. (4-nitrobenzaldehyde) = 107.0 °C, m.p. (4-nitroaniline) = 146.0 °C.

1.2. Milling equipment

Mechanochemical reactions were carried out using a mixer ball mill IST500 (InSolido Zagreb) operating at 30 Hz in either stainless steel (SS) or poly(methyl)methacrylate (PMMA) milling jars, and with stainless-steel milling balls, mass 1.4 g. The milling reactions were monitored by in situ Raman spectroscopy using 14 mL translucent PMMA jars. Raman experiments were performed by the portable Raman system with PD-LD (now Necsel) BlueBox laser source with the 785 nm excitation wavelength, coupled to OceanOptics Maya2000Pro spectrometer.¹

1.3. Nuclear Magnetic Resonance (NMR) spectroscopy

Solution NMR spectra were recorded on an NMR Bruker Avance 600 and 300 MHz using CDCl₃ or DMSO-*d*₆ as solvents and tetramethylsilane (TMS) as an internal reference at 25 °C. Chemical shifts are reported in parts per million (ppm).

Solid-state NMR spectra were acquired on Bruker Avance NEO 400 MHz NMR spectrometer equipped with 4.0 mm dual resonance HX CPMAS iProbe. Larmor frequencies of proton, carbon and nitrogen nuclei were 400, 100 and 40 MHz, respectively. ¹H and ¹³C NMR chemical shifts are reported relative to TMS (δ 0.0 ppm). Chemical shifts were referenced using adamantane as an external reference for tetramethylsilane (TMS), setting the CH₂ signal to 38.48 ppm. ¹⁵N NMR chemical shifts are reported relative to liquid ammonia (δ _N 0.0 ppm). Samples were pressed in a 4.0 mm diameter ZrO₂ rotors and sealed with Kel-F caps. Spinning rates were 15 000 Hz for ¹H MAS, 12 000 Hz for ¹³C CP-MAS and 10 000 Hz for ¹⁵N CP-MAS spectra.

1.4. Powder X-Ray diffraction (PXRD)

Prepared samples were fine powders whose diffractograms were collected on a benchtop Panalytical Aeris diffractometer with Ni-filtered CuK α radiation in Bragg-Brentano geometry using a zero-background sample holder. The copper X-ray tube was operated

at 40 kV and 7.5 mA, while the samples were prepared as thin films on zero-background silicon holders. The PXRD monitoring of mechanochemical reactions was conducted immediately after stopping the mill and sampling the representative part of the reaction mixture for analysis.

1.5. Infrared spectroscopy (IR)

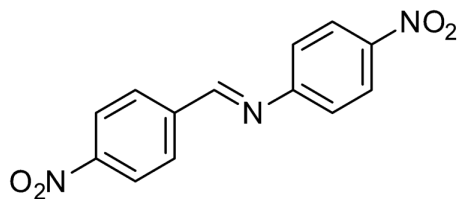
FT-IR spectra of compounds were recorded on PerkinElmer Spectrum Two FT-IR spectrometer (UATR mode). The spectra were analyzed in the sophisticated Perkin Elmer program or in MATLAB.

1.6. Computational details

Calculations were performed using the ω B97xd functional and the standard 6-311+G** basis set as implemented in the Gaussian16.² Stationary points obtained by full geometry optimization were characterized by vibrational analysis as minima (no imaginary frequencies) or transition states (one imaginary frequency). IRC calculations followed by geometry optimization were performed to confirm minima as reactants and products. Calculated Raman spectra were uniformly scaled by a factor 0.95. Energies were reported with regard to the free reactants (**1**) and (**2**) using the correction for amine dimerization in the solid state. Namely, the amine **2** is in the solid state packed *via* $\text{NH}_2 \cdots \text{O}_2\text{N}$ interactions. In an effort to account for this, we used a “dimer” of two molecules of **2** that was calculated to be $16.0 \text{ kcal mol}^{-1}$ more stable than the corresponding non-interacting two molecules of **2**. Our hypothesis was that this “dimer” has to be broken before **2** is engaged in the solid-state reaction.

1.7. Imine synthesis procedure

4-nitrobenzaldehyde **1** (1 mmol, 151 mg) and 4-nitroaniline **2** (1 equiv., 138 mg) were weighed at room temperature in air and placed separately in the PMMA grinding jars loaded with two SS balls, mass 1.4 g. In the jars were also added 0.1 equiv. of listed acid or base additives, unless stated otherwise (see the paper, Table 1). The reaction mixture was generally homogeneous during the experiment, which is important for obtaining high-quality Raman spectra. The milling jar was placed in the mixer mill operating at 30 Hz, and the reaction mixture was milled preliminary for 1 h. The reactions were monitored by thin-layer chromatography on silica gel 60 F254 aluminum sheets. After milling crude samples without further purification were sent for ^1H NMR analysis. If the grinding was performed overnight, due to the visible contamination with iron from SS balls, the reaction mixture was diluted in dichloromethane, filtered over Celite and evaporated under vacuum.



(*E*)-4-nitro-*N*-(4-nitrobenzylidene)aniline (**3**): **3** was isolated as a yellow solid (271.23 g/mol, 98%). Characterization data are consistent with the previously published data:³ ¹H NMR (300 MHz, DMSO-*d*₆), δ / ppm: 8.85 (s, 1H), 8.40 (d, *J* = 8.6 Hz, 2H), 8.33 (d, *J* = 8.8 Hz, 2H), 8.23 (d, *J* = 8.7 Hz, 2H), 7.52 (d, *J* = 8.8 Hz, 2H).

2. Figures

2.1. Raman

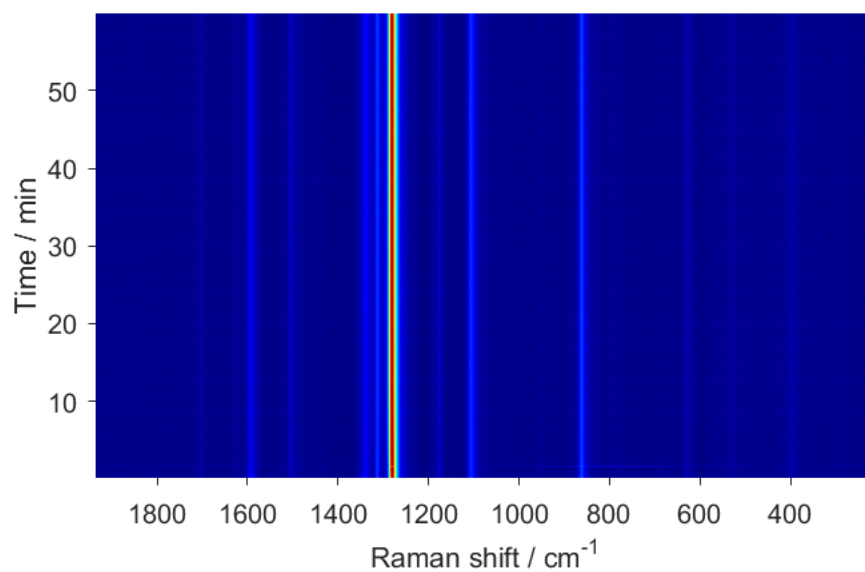


Figure S1. 2D plot of time-resolved Raman monitoring of **1** (1 mmol) and **2** (1 mmol) under dry conditions for 60 min.

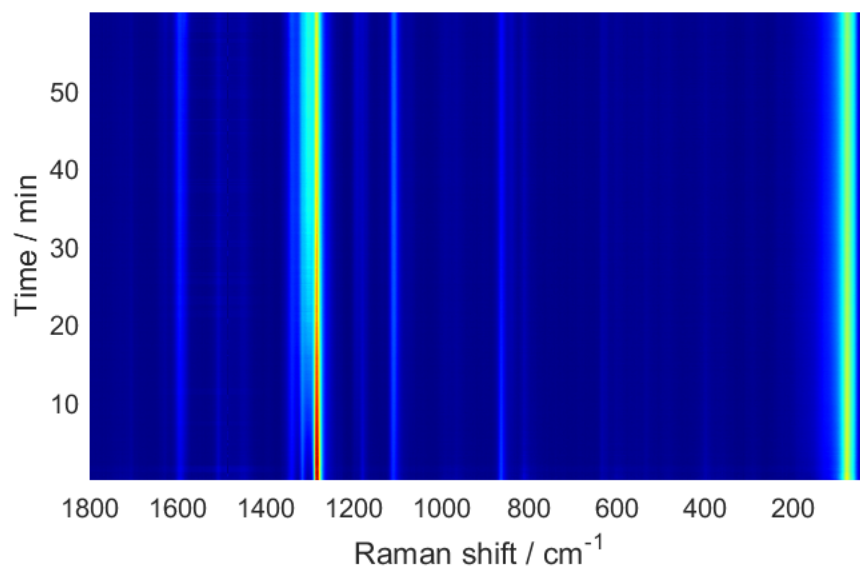


Figure S2. 2D plot of the time-resolved Raman monitoring of **1** (1 mmol) and **2** (1 mmol) with acetic acid (0.1 equiv.) during 60 min of grinding.

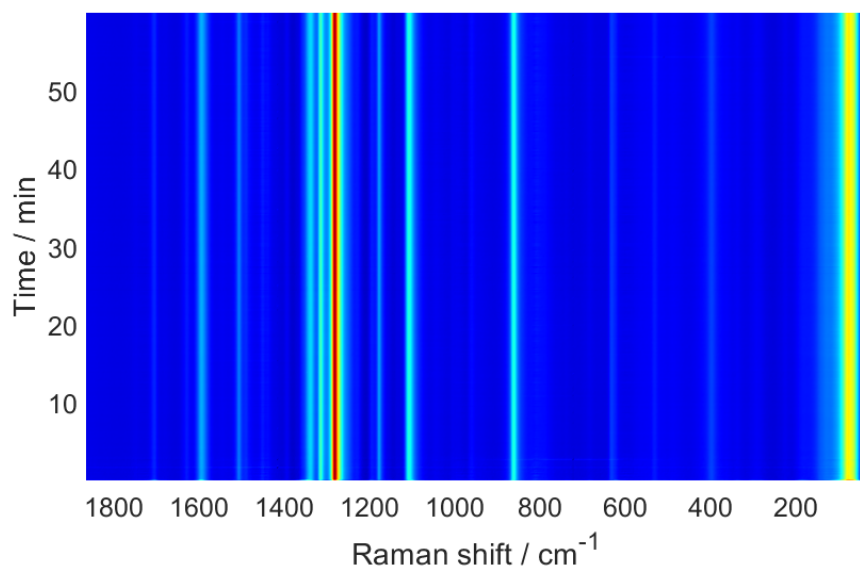


Figure S3. 2D plot of the time-resolved Raman monitoring of **1** (1 mmol) and **2** (1 mmol) with DMF (0.1 equiv.) during 60 min of grinding. The same plot was observed when aluminum oxide was added to the reaction mixture as a filler to prevent sticking of the milled material to the jar walls.

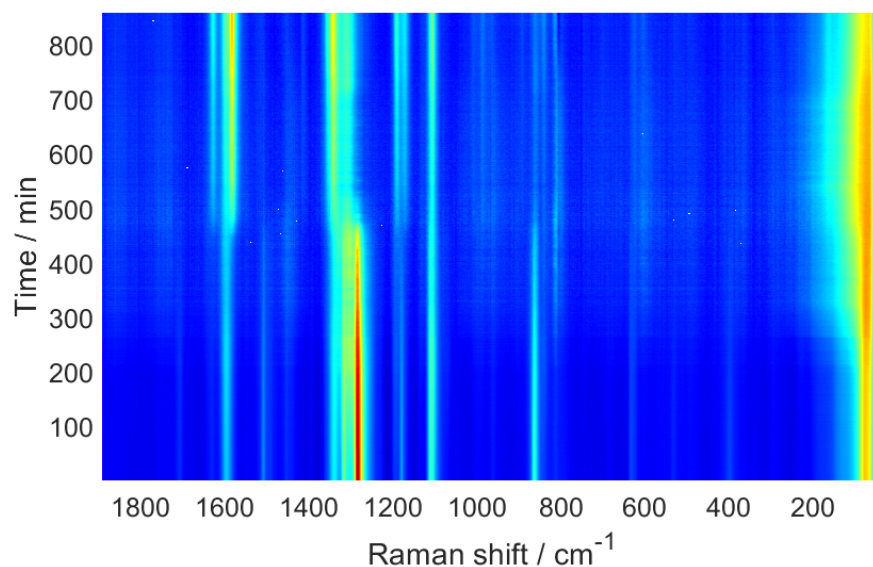


Figure S4. 2D plot of the time-resolved Raman monitoring of **1** (1 mmol) and **2** (1 mmol) with DMF (0.1 equiv.) during overnight grinding. There seems to be something happening before the imine starts to form just before 500 minutes of milling have passed. This is visible with the reduction in the aniline signal and in the phonon region of the spectra.

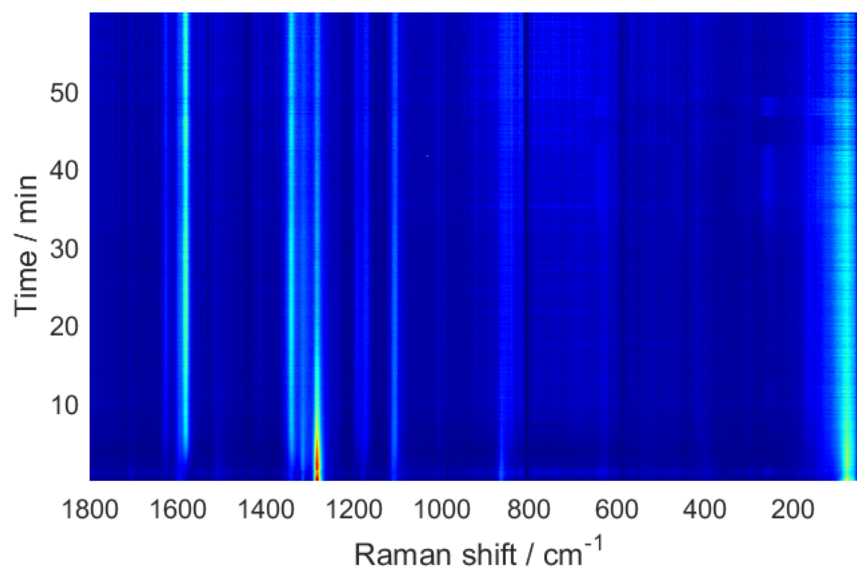


Figure S5. 2D plot of the time-resolved Raman monitoring of **1** (1 mmol) and **2** (1 mmol) with DBU (0.1 equiv.) during 60 min of grinding.

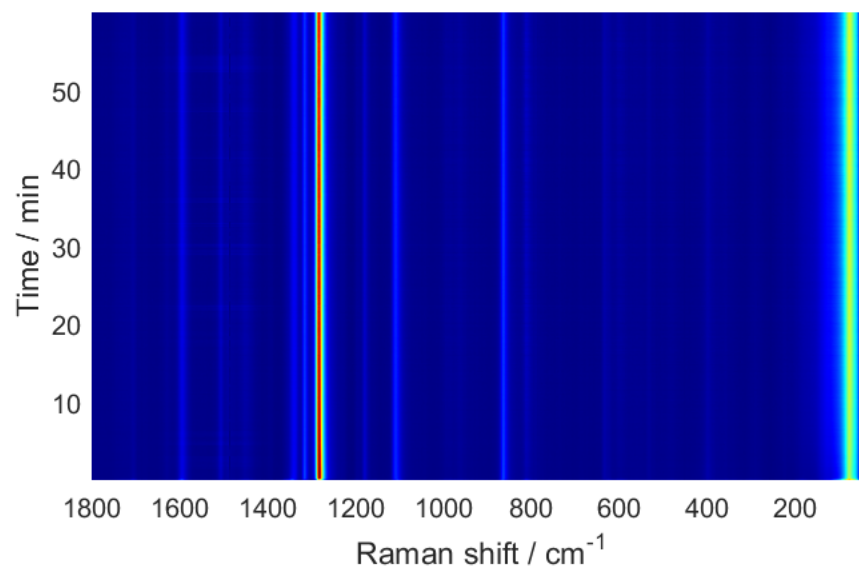


Figure S6. 2D plot of the time-resolved Raman monitoring of **1** (1 mmol) and **2** (1 mmol) with Et₂O (0.1 equiv.) during 60 min of grinding.

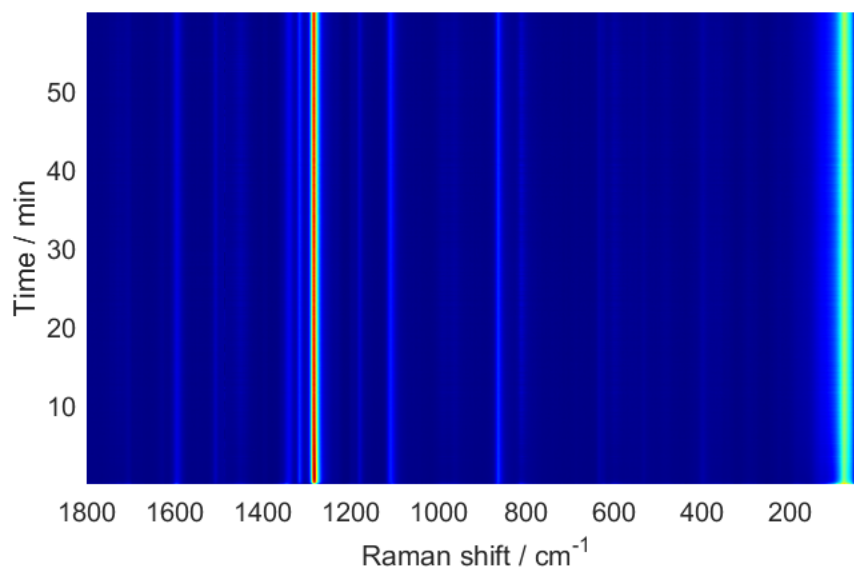


Figure S7. 2D plot of the time-resolved Raman monitoring of **1** (1 mmol) and **2** (1 mmol) with n-heptane (0.1 equiv.) during 60 min of grinding.

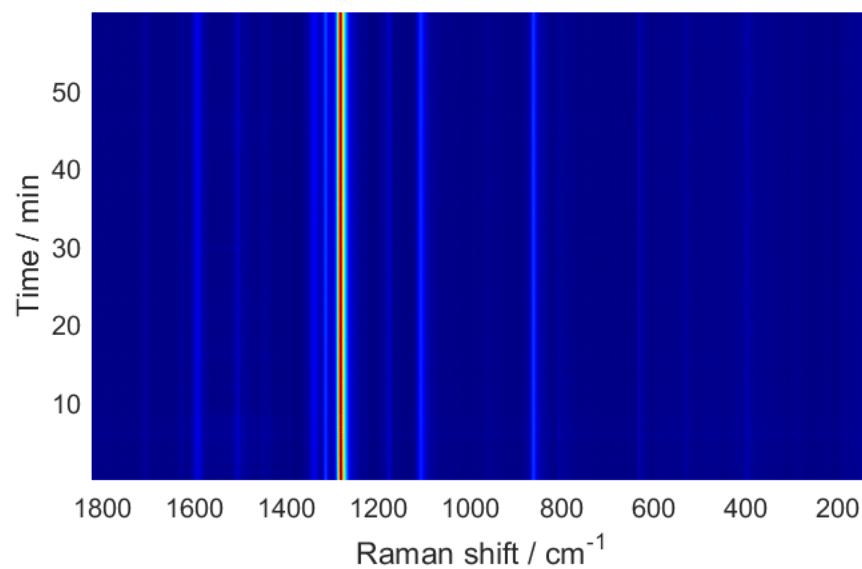


Figure S8. 2D plot of the time-resolved Raman monitoring of **1** (1 mmol) and **2** (1 mmol) with distilled water (0.1 equiv.) during 60 min of grinding.

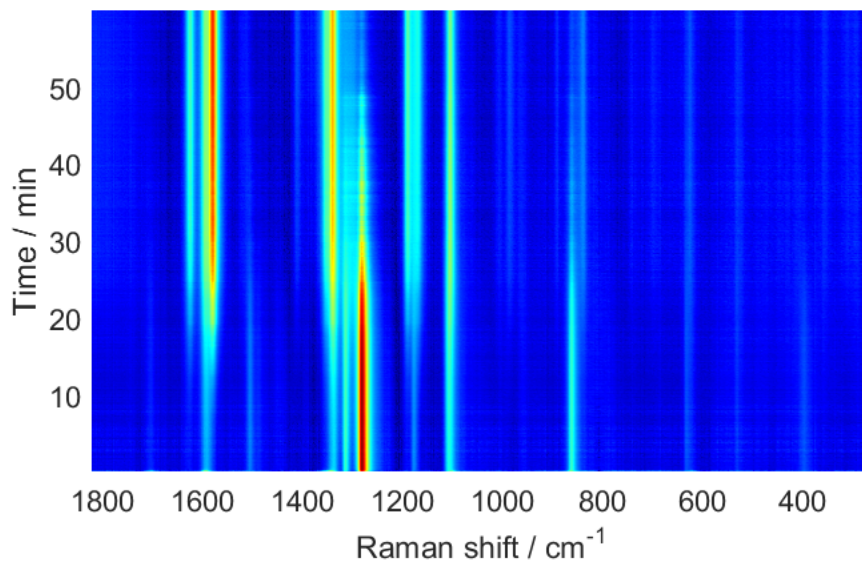


Figure S9. 2D plot of the time-resolved Raman monitoring of **1** (1 mmol) and **2** (1 mmol) with sulfamic acid (0.1 equiv.) during 60 min of grinding.

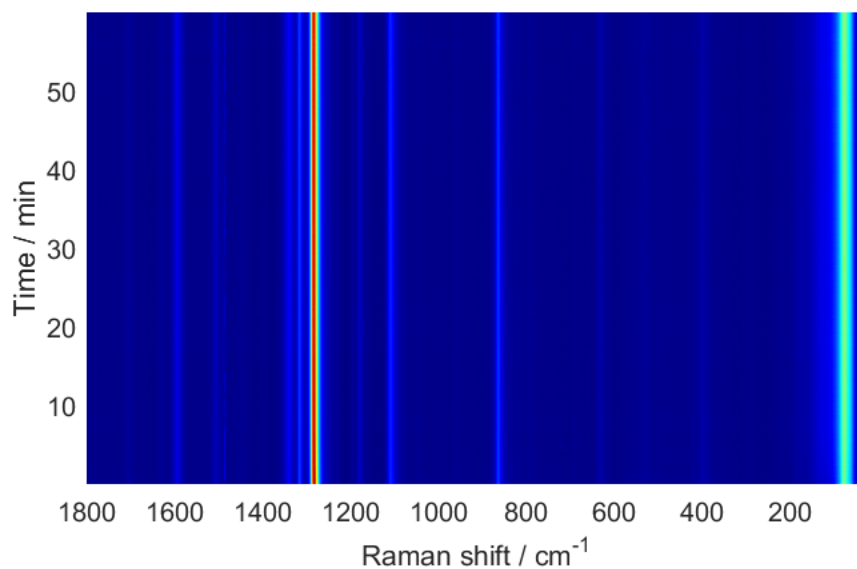


Figure S10. 2D plot of the time-resolved Raman monitoring of **1** (1 mmol) and **2** (1 mmol) with acetonitrile (0.1 equiv.) during 60 min of grinding.

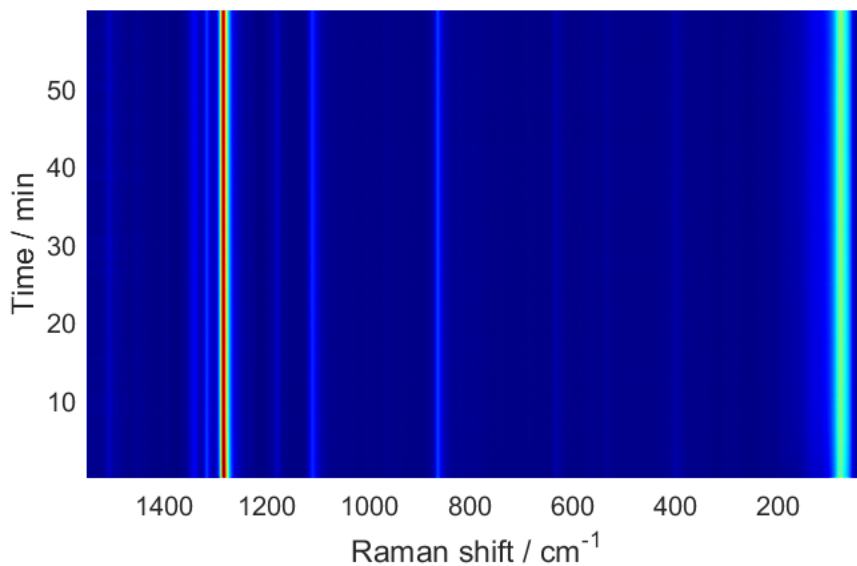


Figure S11. 2D plot of the time-resolved Raman monitoring of **1** (1 mmol) with **2** (1 mmol) and methanol (0.1 equiv.) during 60 min of grinding.

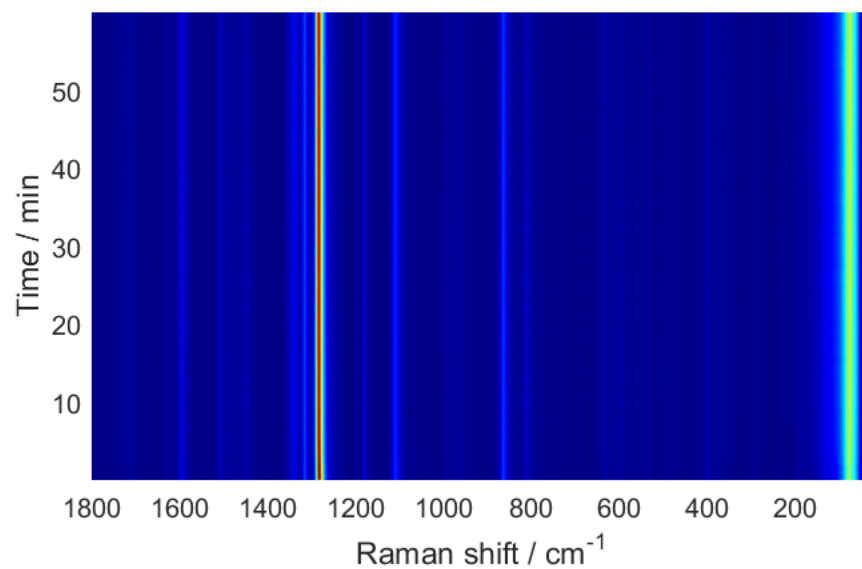


Figure S12. 2D plot of the time-resolved Raman monitoring of **1** (1 mmol) with **2** (1 mmol) and 2-propanol (0.1 equiv.) during 60 min of grinding.

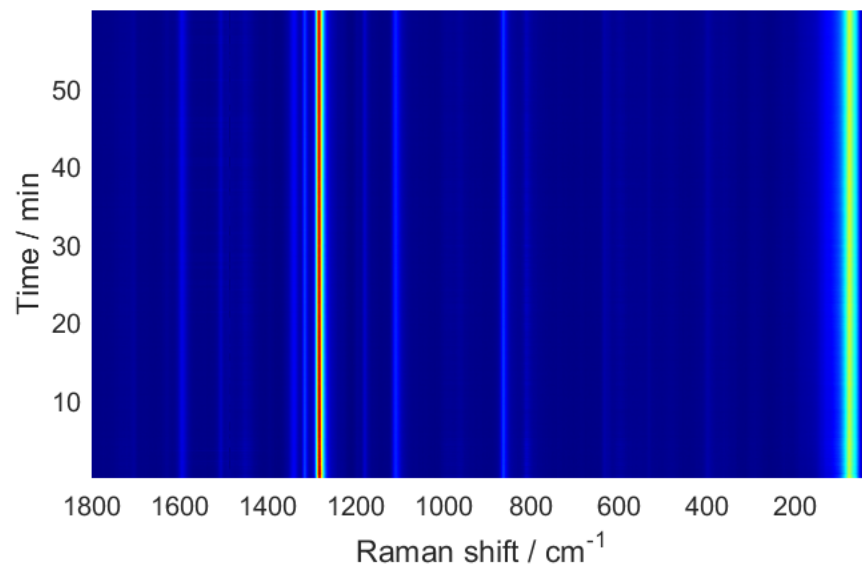


Figure S13. 2D plot of the time-resolved Raman monitoring of **1** (1 mmol) with **2** (1 mmol) and nitromethane (0.1 equiv.) during 60 min of grinding.

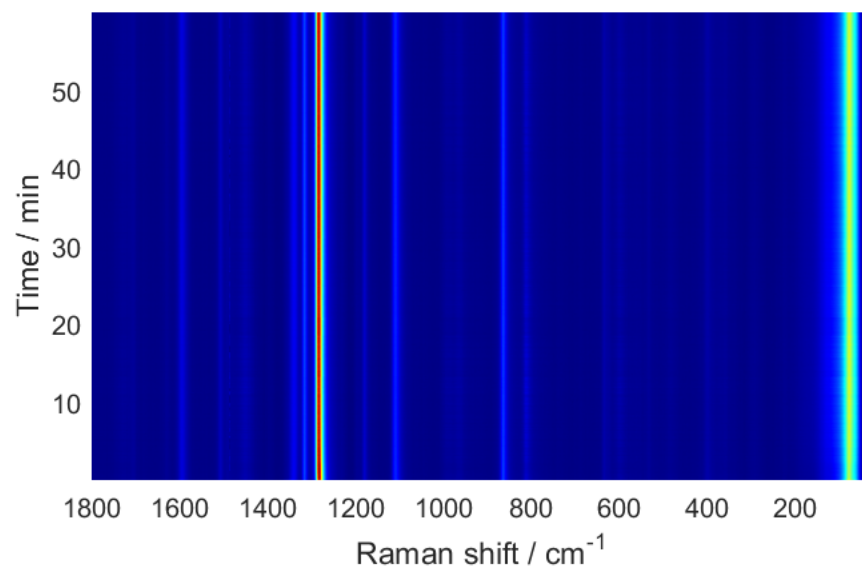


Figure S14. 2D plot of the time-resolved Raman monitoring of **1** (1 mmol) with **2** (1 mmol) and acetone (0.1 equiv.) during 60 min of grinding.

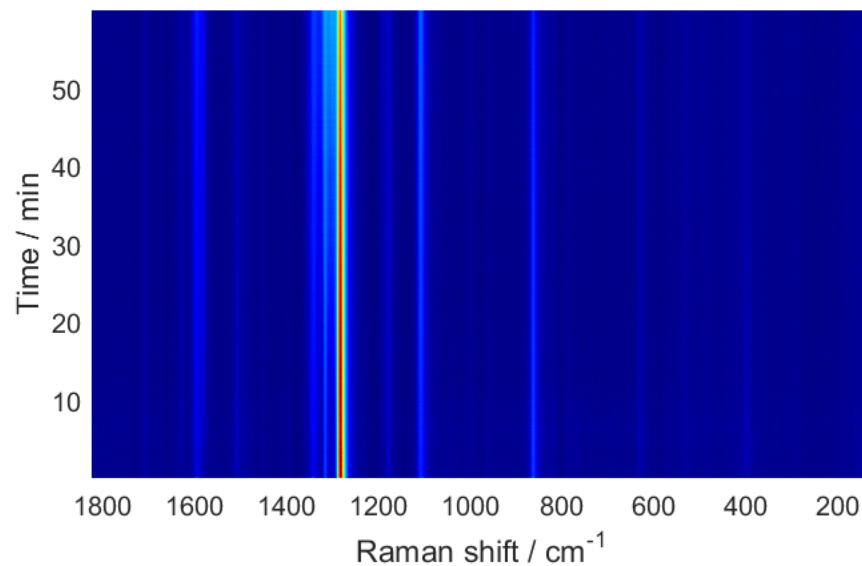


Figure S15. 2D plot of the time-resolved Raman monitoring of **1** (1 mmol) with **2** (1 mmol) and benzoic acid (0.1 equiv.) during 60 min of grinding.

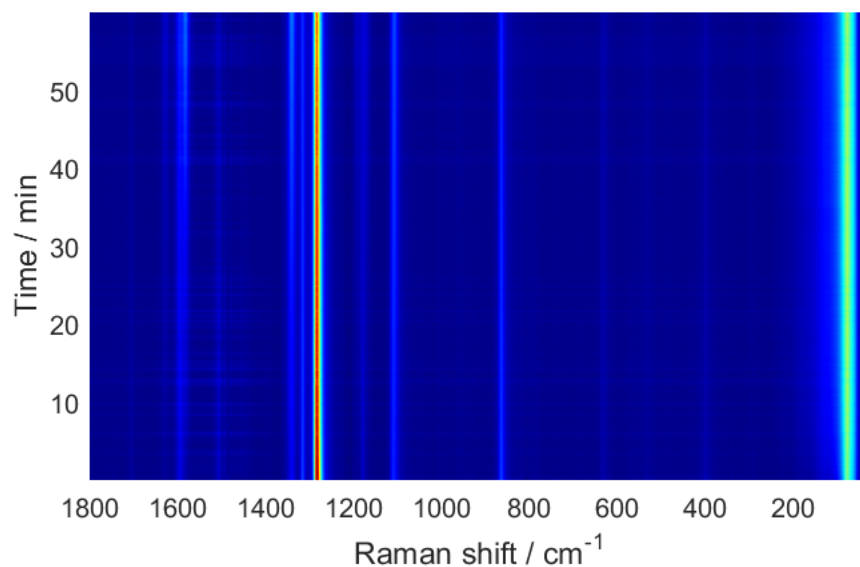


Figure S16. 2D plot of the time-resolved Raman monitoring of **1** (1 mmol) with **2** (1 mmol) and methacrylic acid (0.1 equiv.) during 60 min of grinding.

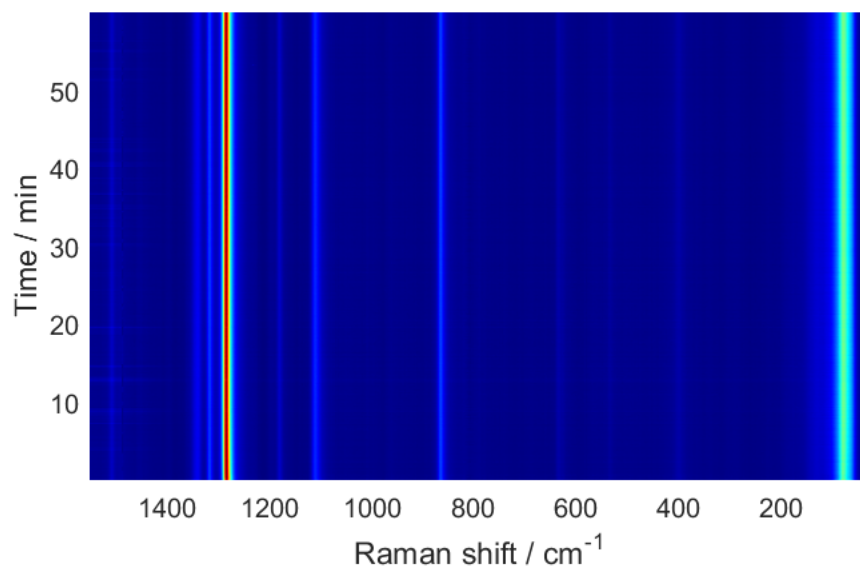


Figure S17. 2D plot of the time-resolved Raman monitoring of **1** (1 mmol) with **2** (1 mmol) and triethylamine (0.1 equiv.) during 60 min of grinding.

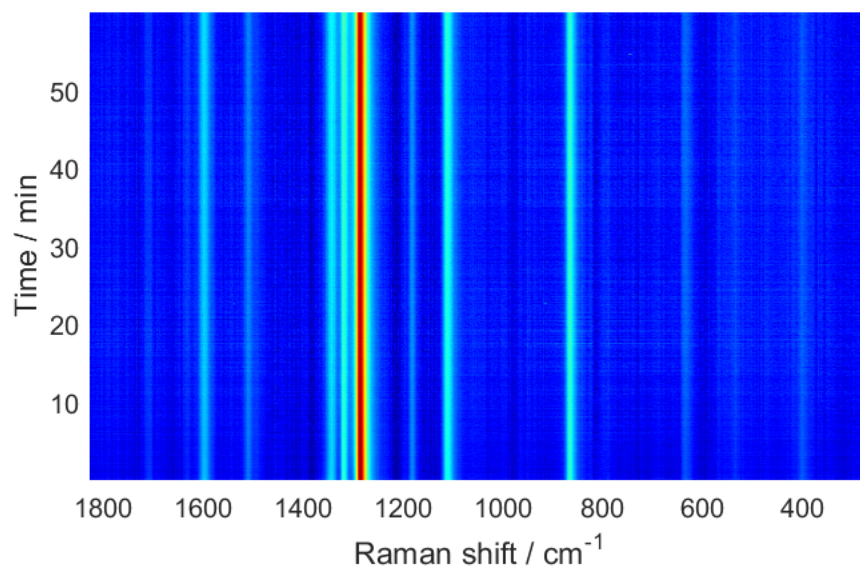


Figure S18. 2D plot of the time-resolved Raman monitoring of **1** (1 mmol) with **2** (1 mmol) and ammonium acetate (0.1 equiv.) during 60 min of grinding.

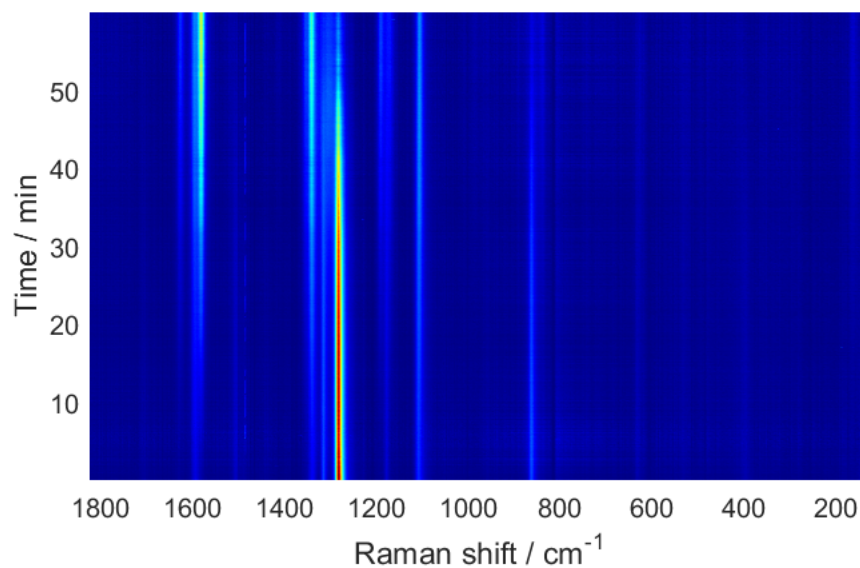


Figure S19. 2D plot of the time-resolved Raman monitoring of **1** (1 mmol) with **2** (1 mmol) and zeolite, CBV-760 (0.1 equiv.) during 60 min of grinding.

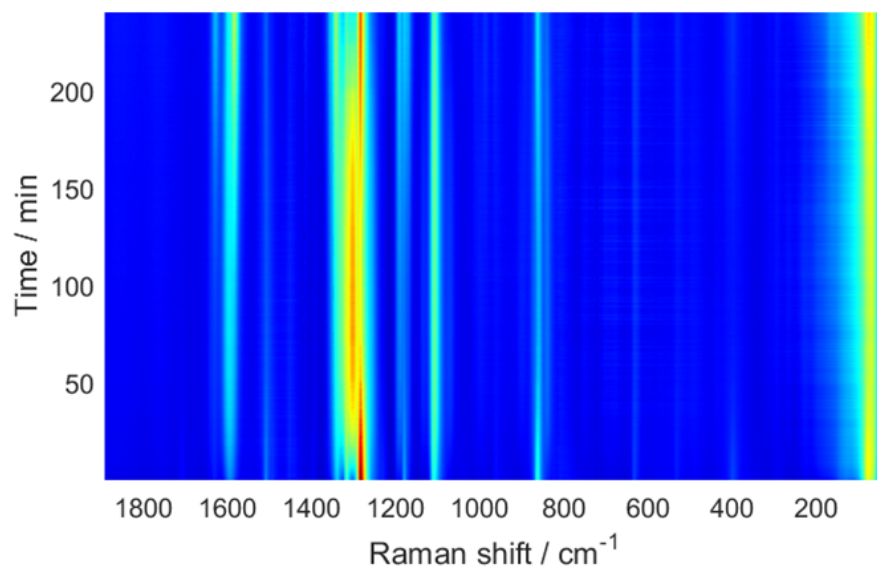


Figure S20. 2D plot of the time-resolved Raman monitoring of **1** (1 mmol) and **2** (1 mmol) in a molar ratio 1:2 with AcOH (0.1 equiv.) during 240 min.

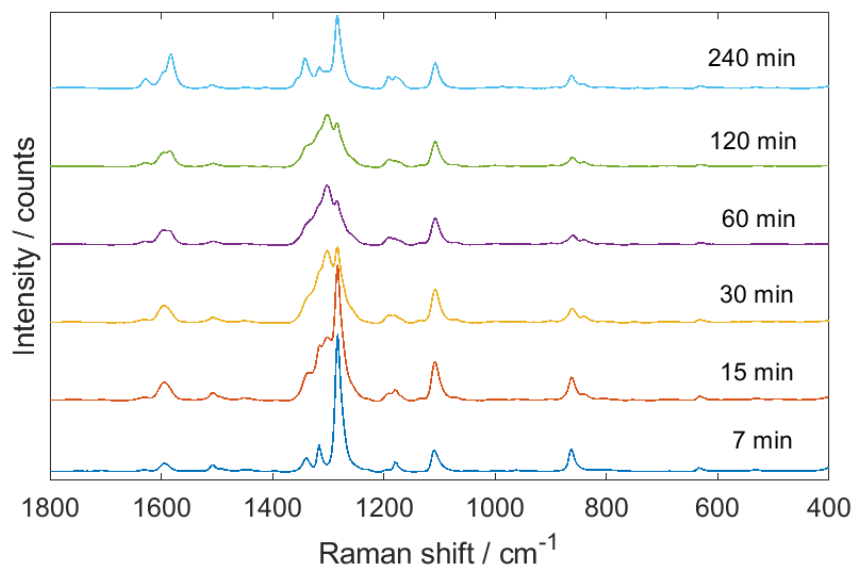


Figure S21. Raman spectra collected during 240 min of grinding **1** and **2** in a molar ratio 1:2 with the addition of 0.1 equiv. of acetic acid.

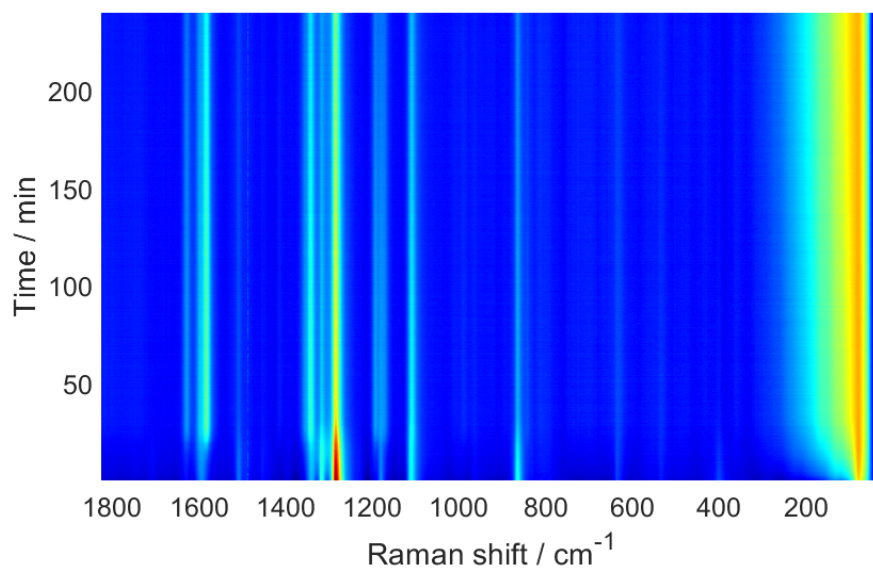


Figure S22. 2D plot of the time-resolved Raman monitoring of **1** (1 mmol) and **2** (1 mmol) in a molar ratio 1:2 with SA (0.1 equiv.) during 240 min of grinding.

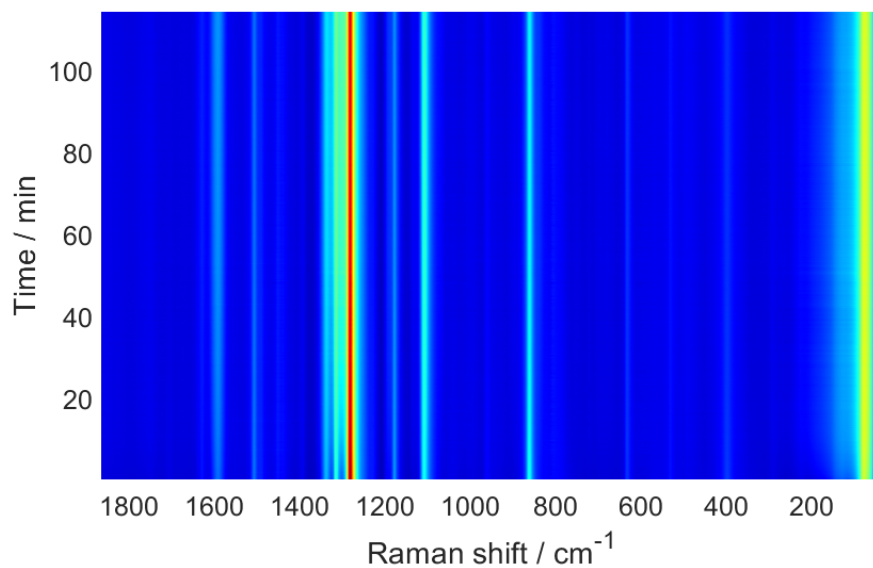


Figure S23. 2D plot of the time-resolved Raman monitoring of **1** (1 mmol) and **2** (1 mmol) in a molar ratio 1:5 with AcOH (0.1 equiv.).

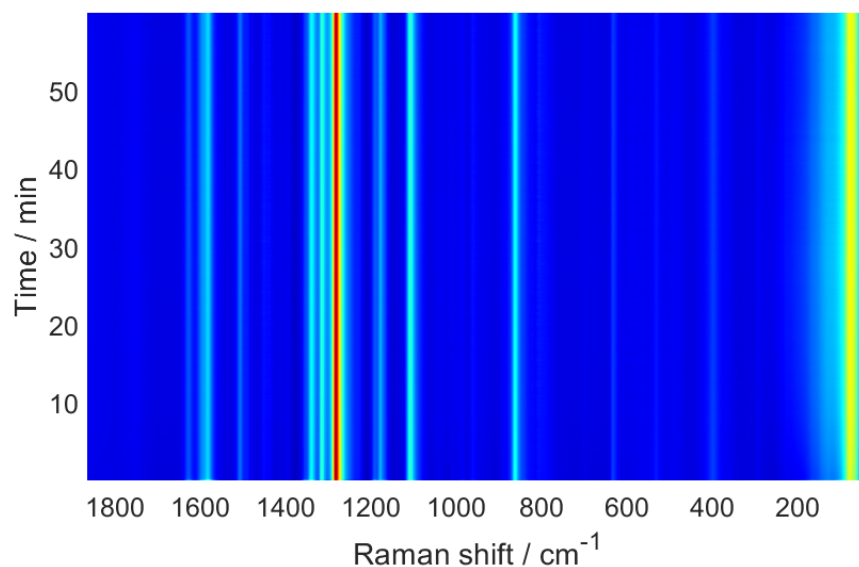


Figure S24. 2D plot of the time-resolved Raman monitoring of **3** (1 mmol) and **2** (1 mmol) in a molar ratio 1:5 with AcOH (0.1 equiv.).

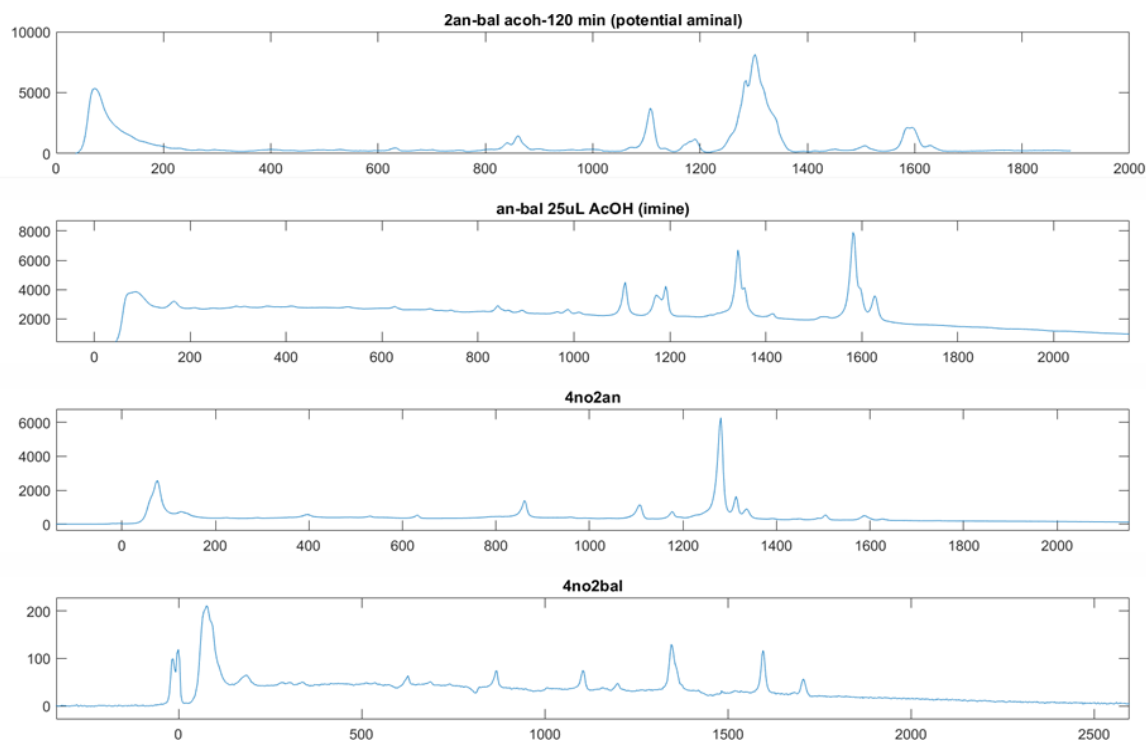


Figure S25. Comparison of experimental Raman spectra of starting materials (bottom), imine and the potential aminal (**5**) (top). The Raman spectrum of the **5** was extracted from monitoring the reaction between **1** and **2** in a ratio 1:2 with 0.1 equiv. of acetic acid, after 120 min of grinding.

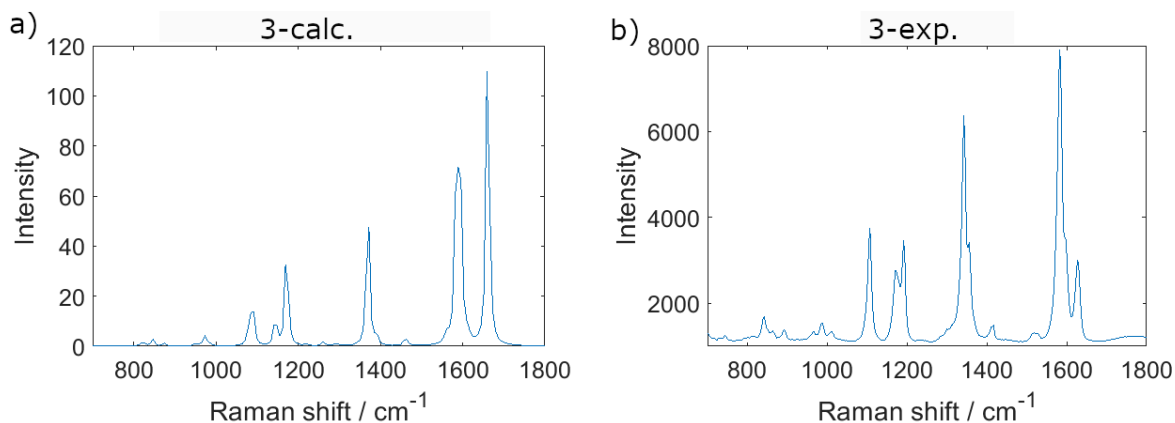


Figure S26. Comparison of (a) calculated and (b) experimental Raman spectra of **3**.

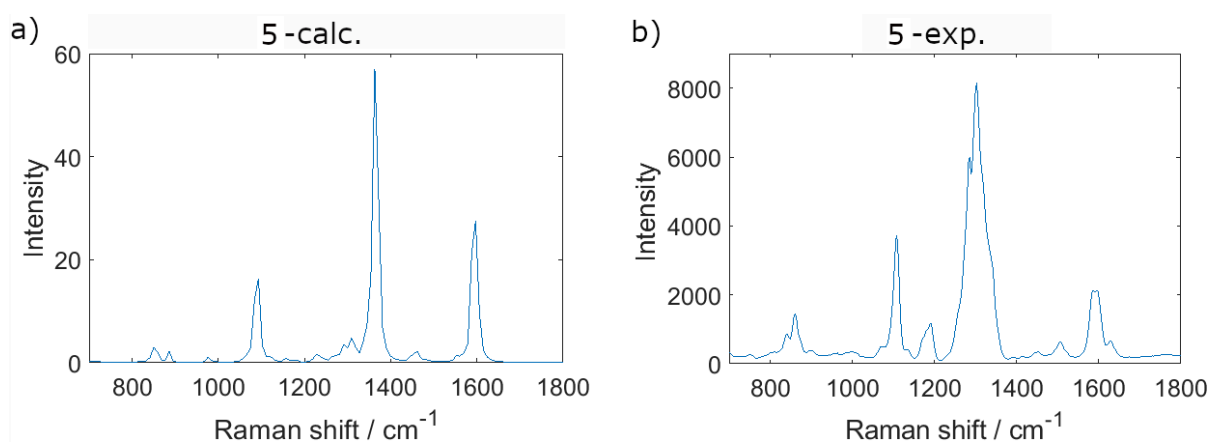


Figure S27. Comparison of (a) calculated and (b) experimental Raman spectra of the **5**.

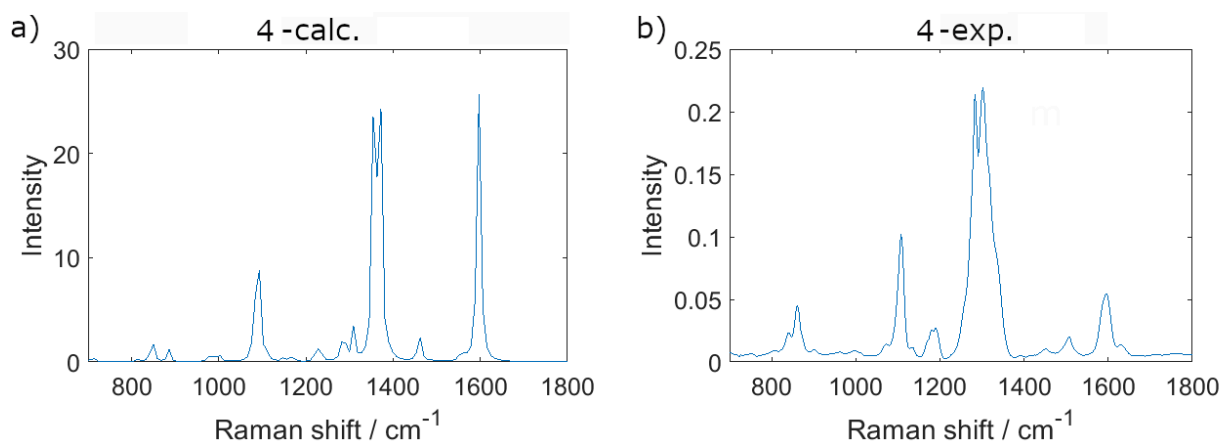


Figure S28. Comparison of (a) calculated and (b) experimental Raman spectra of the hemiaminal (**4**).

2.2. PXRD

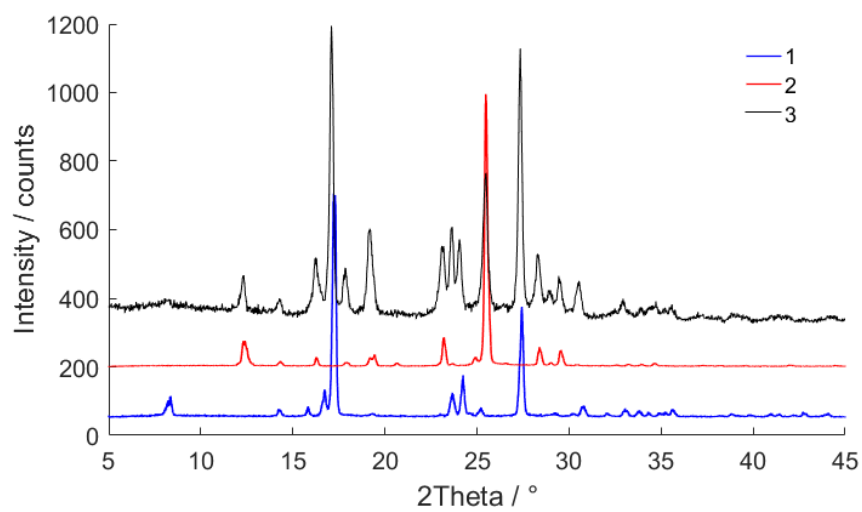


Figure S29. Comparison of the starting materials and the reaction mixture (black line), sampled after neat grinding of **1** and **2** and analyzed *ex-situ* by PXRD.

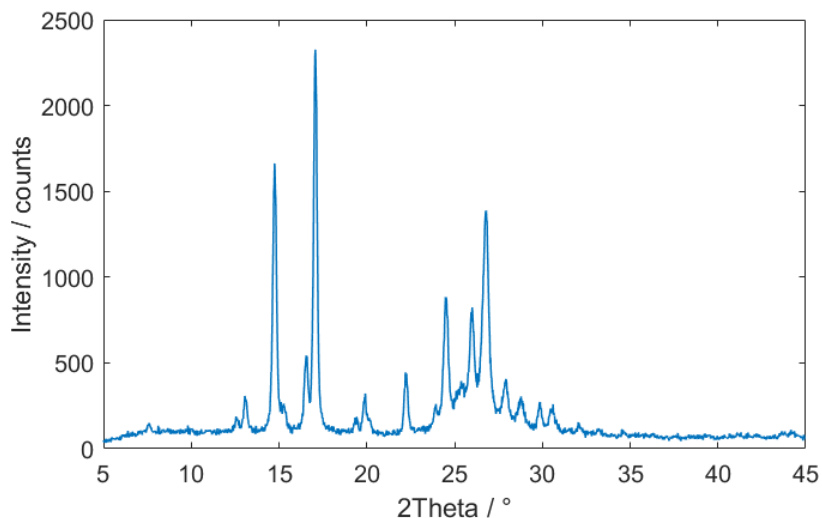


Figure S30. Powder diffractogram of imine **3**. Equimolar amounts of starting materials (1 mmol) with acetic acid as an additive (25 μ L) were milled at 30 Hz for 2 h using a 14 mL PMMA milling jar with two stainless steel milling balls weighing 1.4 g.⁴

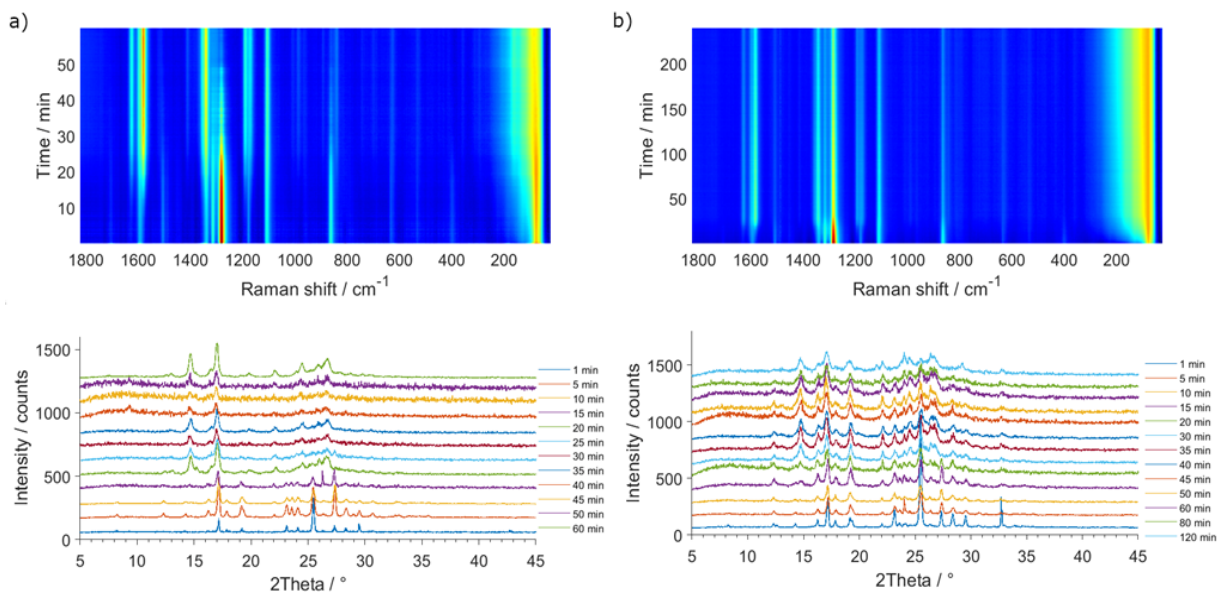


Figure S31. Monitoring of the reaction by in situ Raman spectroscopy (top) and PXRD (bottom) when **1** and **2** are added in a molar ratio: a) 1:1 and b) 1:2, with sulfamic acid (0.1 equiv.). This additive was chosen because of its solid aggregation state, which prevents material loss by evaporation upon frequent opening of the jar for sampling. The starting materials were milled at 30 Hz for 60 min and 240 min using a 14 mL PMMA milling jar with two stainless steel milling balls weighing 1.4 g.

2.3. IR

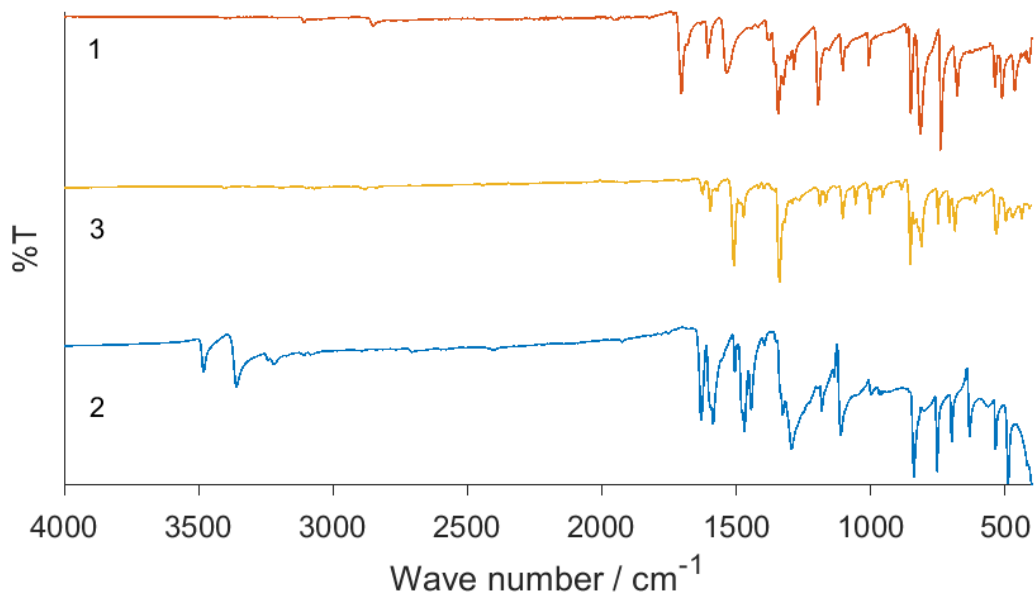


Figure S32. Comparison of IR spectra of the starting materials and the reaction mixture sampled after neat grinding of **1** and **2**.

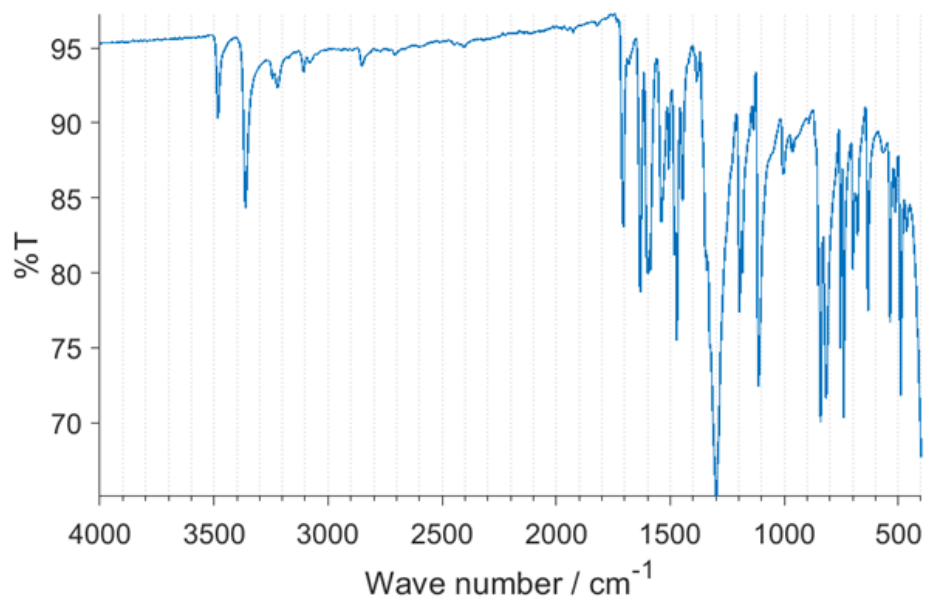


Figure S33. IR spectrum of the sample obtained immediately after 60 min of grinding **1** and **2** in a ratio 1:1, with 0.1 equiv. of DMF.

2.4. NMR

Table S1. ^1H NMR data (DMSO- d_6) for compounds **1-5**.^a

		Compound			
		1	2	3	5
Proton	a	8.41 ppm, d, $J = 8.7$ Hz, 2 H	-	8.40 ppm, d, $J = 8.6$ Hz, 2H	8.34 ppm, d, 2H
	b	8.16 ppm, d, $J = 8.8$ Hz, 2H	-	8.23 ppm, d, $J = 8.7$ Hz, 2H	7.86 ppm, d, 2H
	c	10.17 ppm, s, 1H	-	8.85 ppm, s, 1H	6.45 ppm, t, 1H
	d	-	7.95 ppm, d, $J = 9.1$ Hz, 2H	8.33 ppm, d, $J = 8.8$ Hz, 2H	8.04 ppm, d, 4H
	e	-	6.60 ppm, d, $J = 9.2$ Hz, 2H	7.52 ppm, d, $J = 8.8$ Hz, 2H	6.80 ppm, d, 4H
	f	-	6.71, ppm, s, 2H	-	8.09 ppm, d, 2H

^a s – singlet, d – doublet, t - triplet

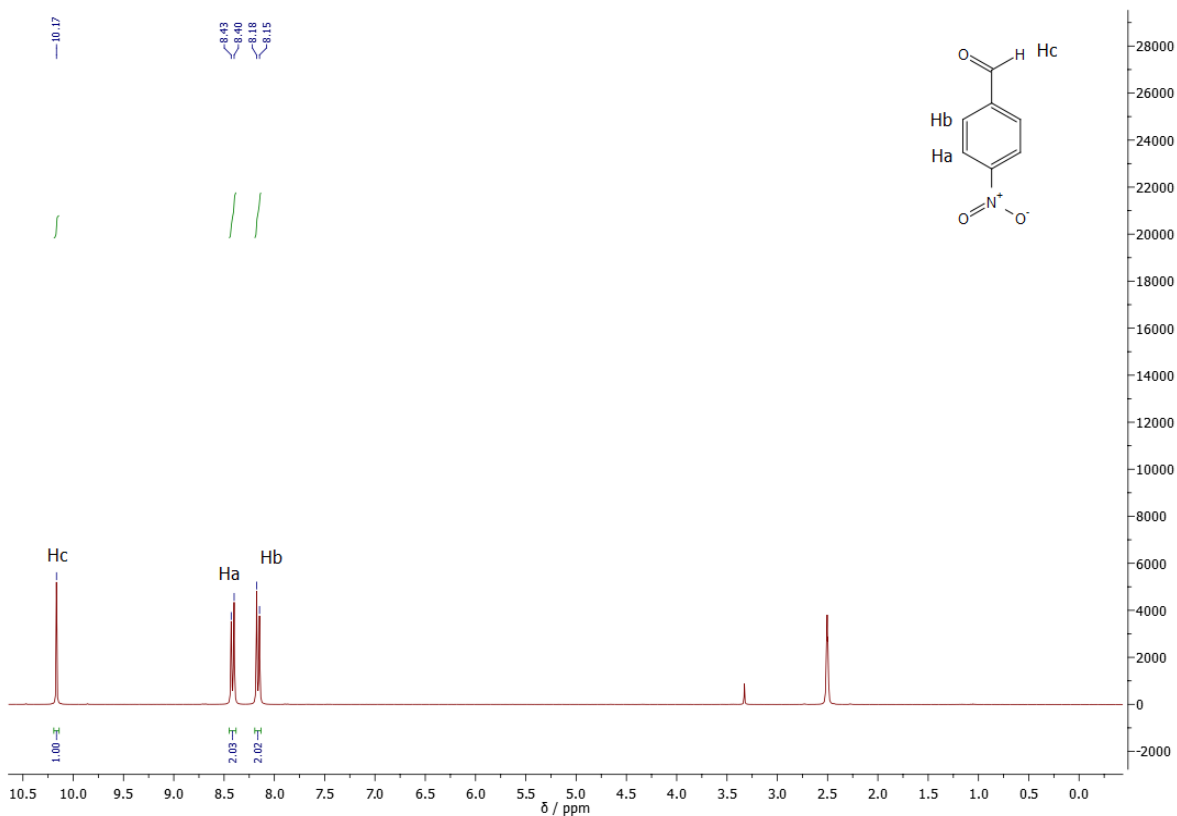


Figure S34. ^1H NMR spectrum of the *p*-nitrobenzaldehyde in DMSO- d_6 (300 MHz).

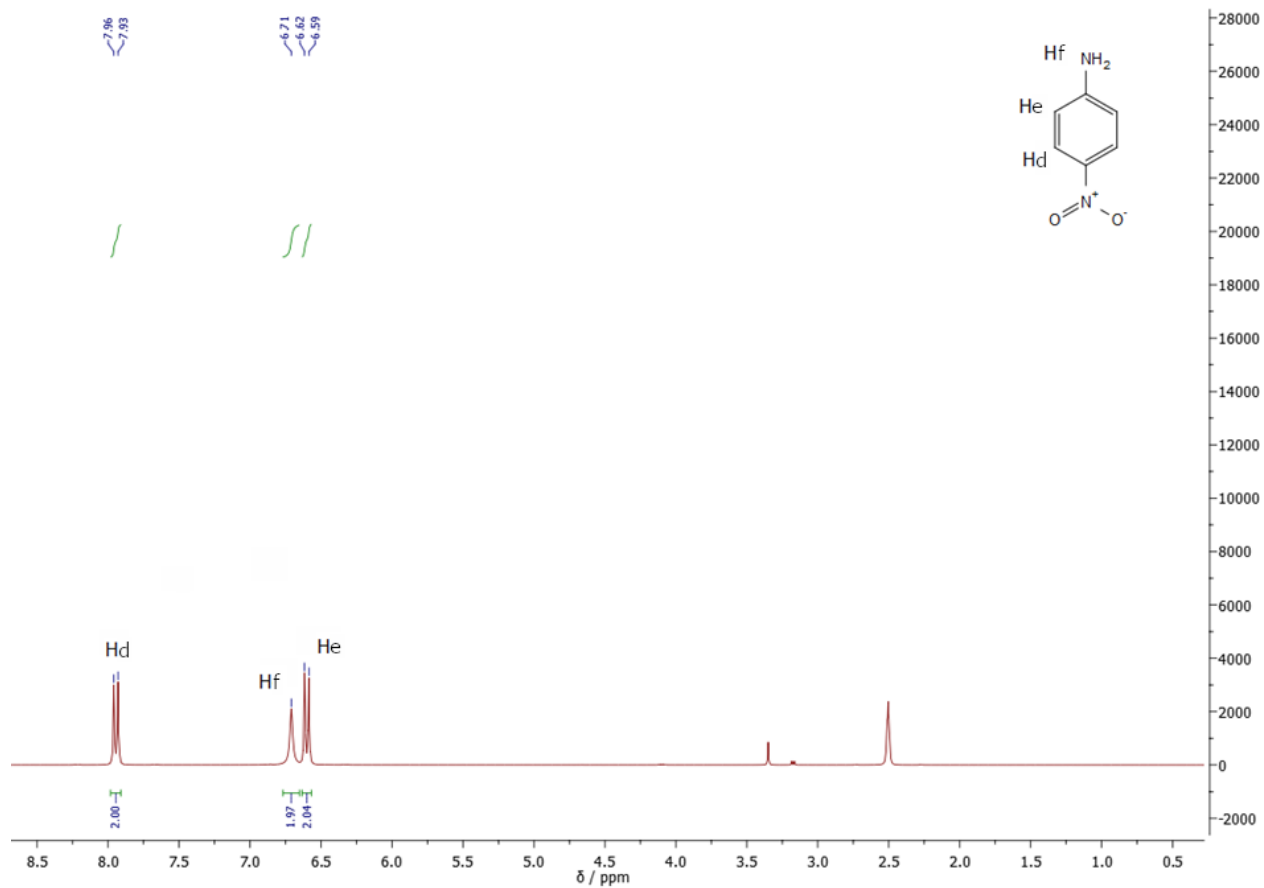


Figure S35. ^1H NMR spectrum of *p*-nitroaniline in $\text{DMSO-}d_6$ (300 MHz).

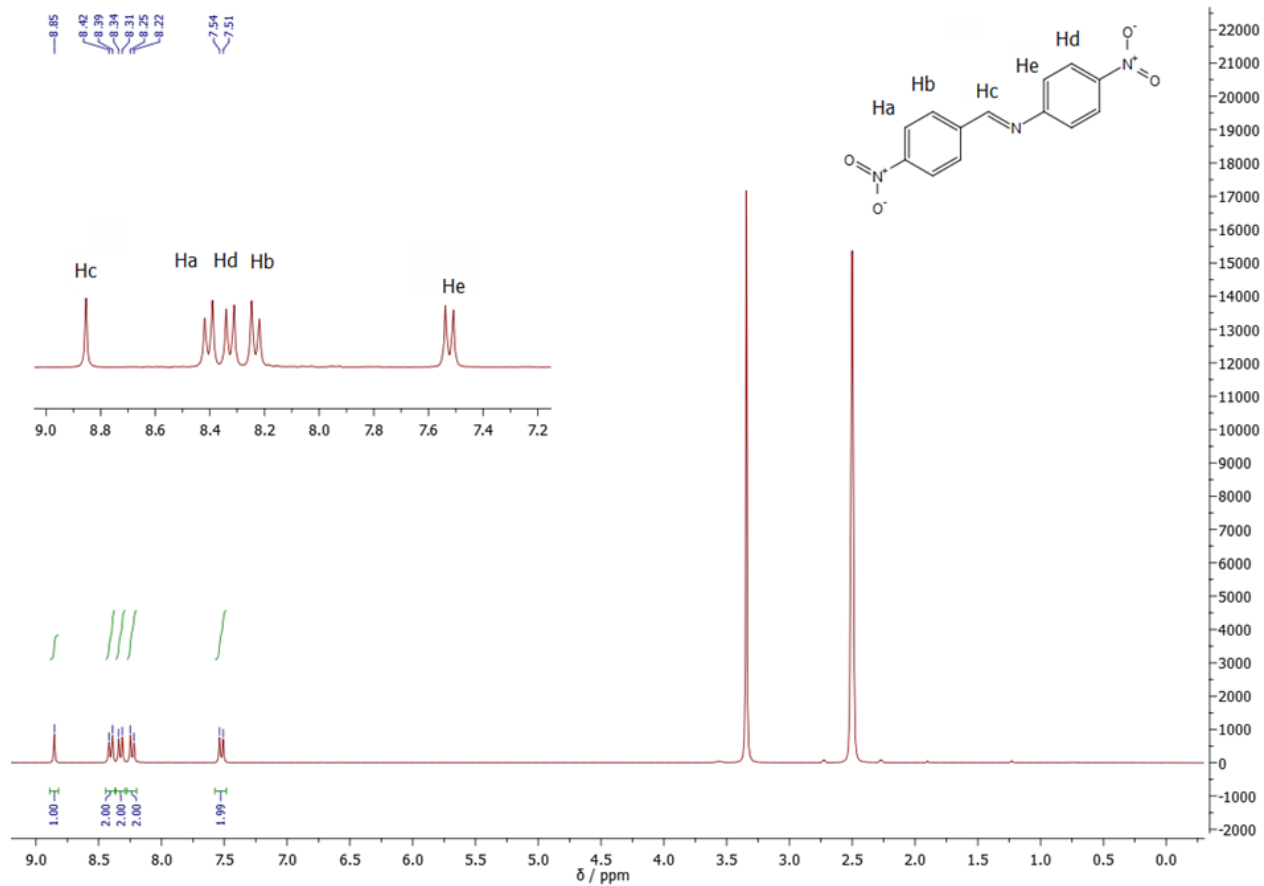


Figure S36. ^1H NMR spectrum of pure imine **3** in $\text{DMSO-}d_6$ (300 MHz).

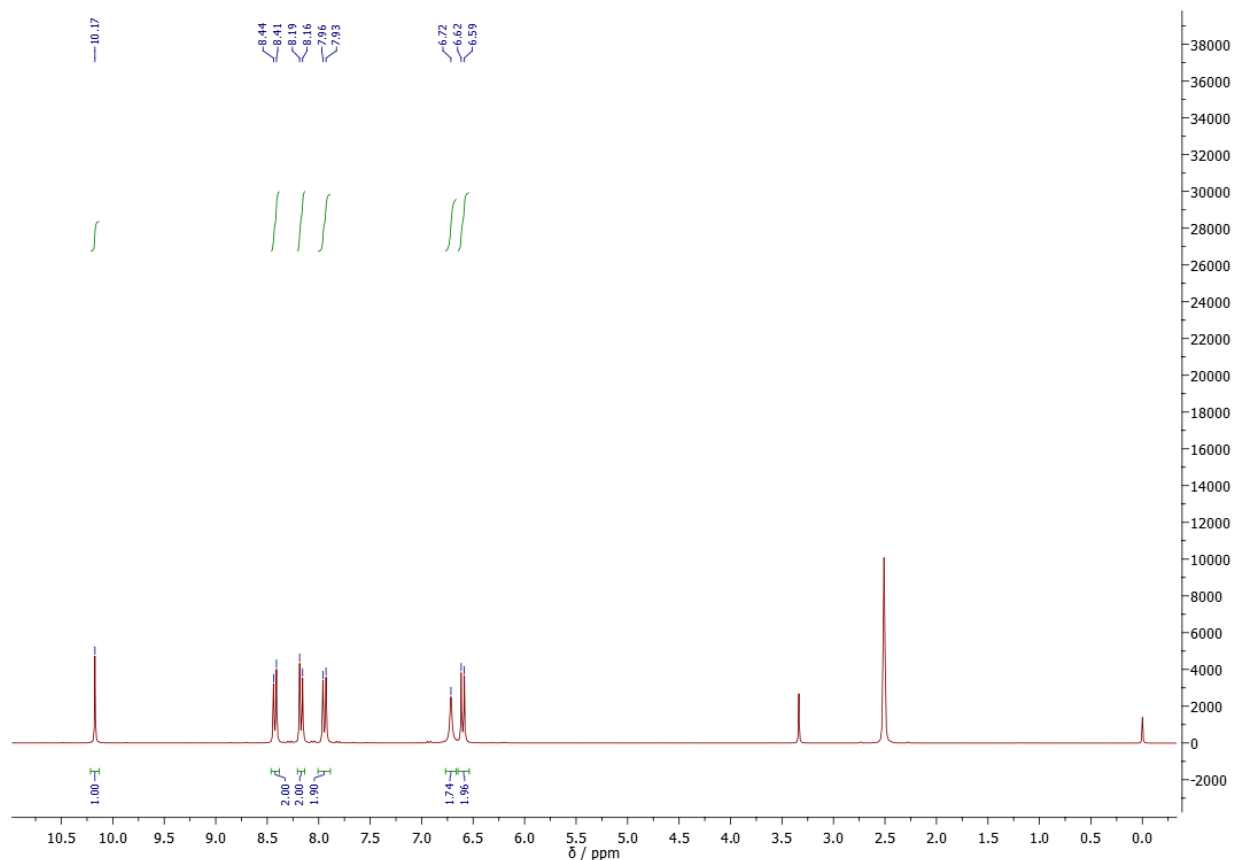


Figure S37. ^1H NMR spectrum of the reaction mixture obtained by grinding **1** and **2** with tungsten carbide balls (3.9 g) for 24 h (DMSO- d_6 , 300 MHz).

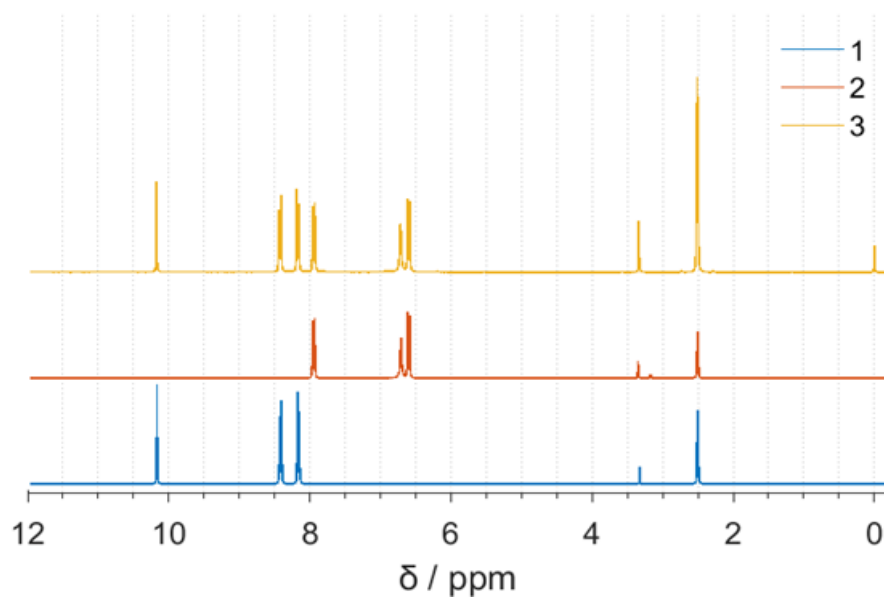


Figure S38. Comparison of ^1H NMR spectra (DMSO- d_6 , 300 MHz) of starting materials **1** and **2** and the reaction mixture sampled after neat grinding for 24 h of **1** and **2**.

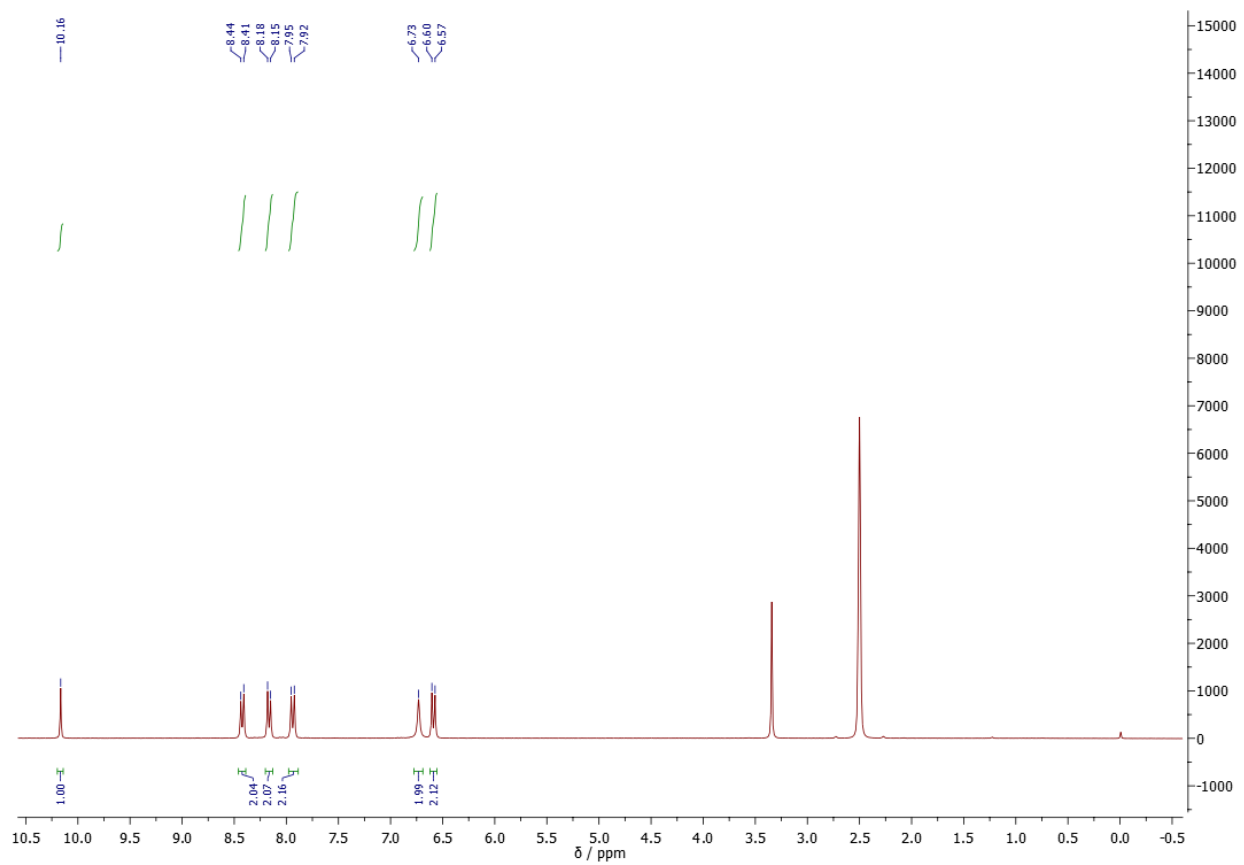


Figure S39. ^1H NMR spectrum of the reaction mixture obtained by grinding **1** and **2** with MeCN as an additive (DMSO- d_6 , 300 MHz).

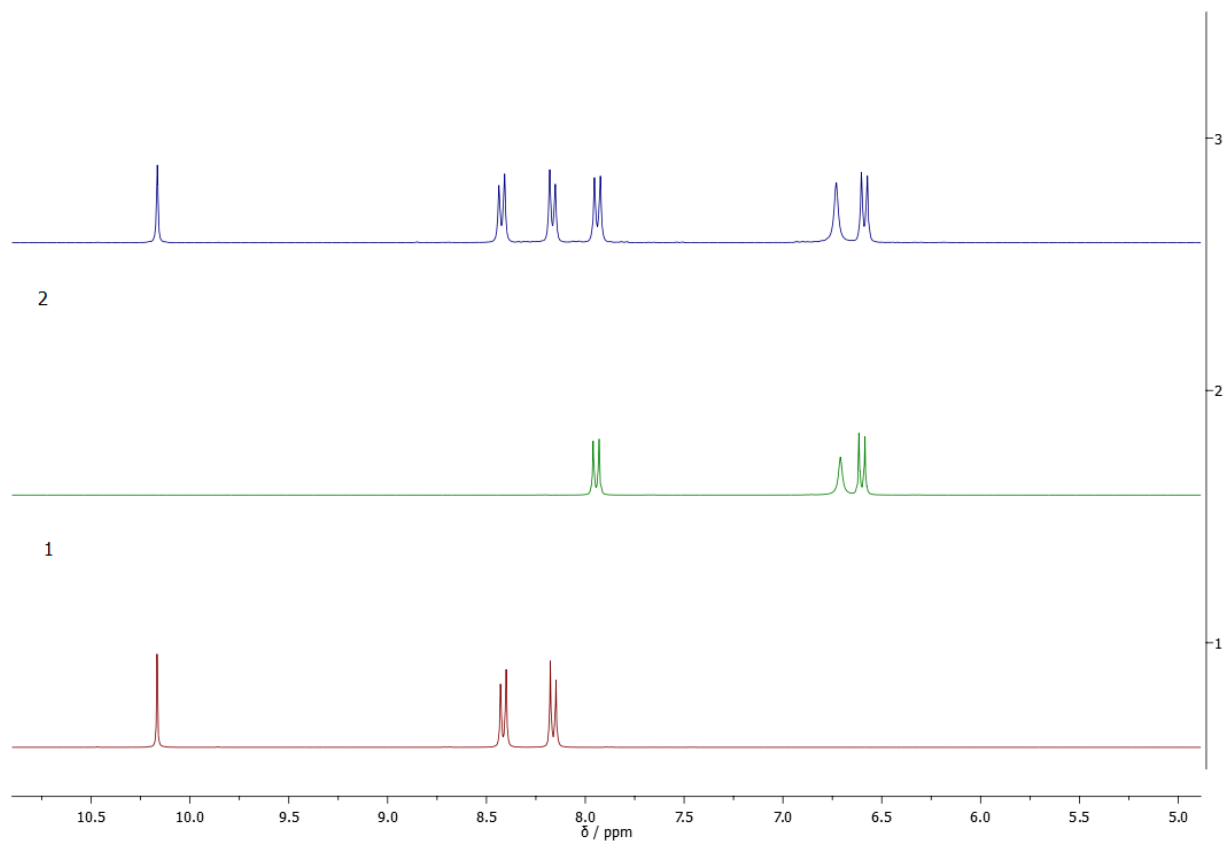


Figure S40. Comparison of ¹H NMR spectra (DMSO-*d*₆, 300 MHz) of starting materials **1** and **2** with the reaction mixture sampled after the reaction with MeCN as an additive (top, blue line).

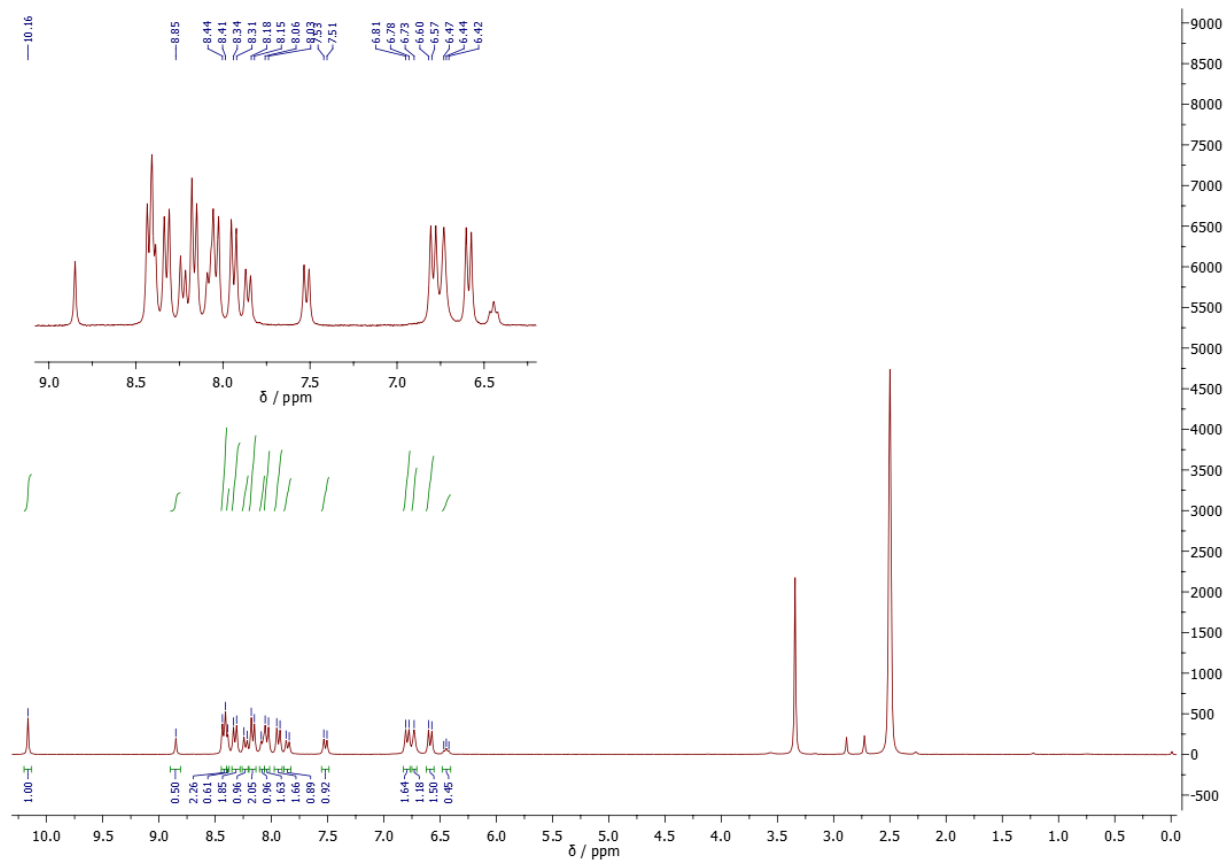


Figure S41. ^1H NMR spectrum of the reaction mixture obtained by grinding **1** and **2** with DMF (0.1 equiv.) during 60 min ($\text{DMSO-}d_6$, 300 MHz). The mixture was standing for 3 days before recording the NMR spectrum.

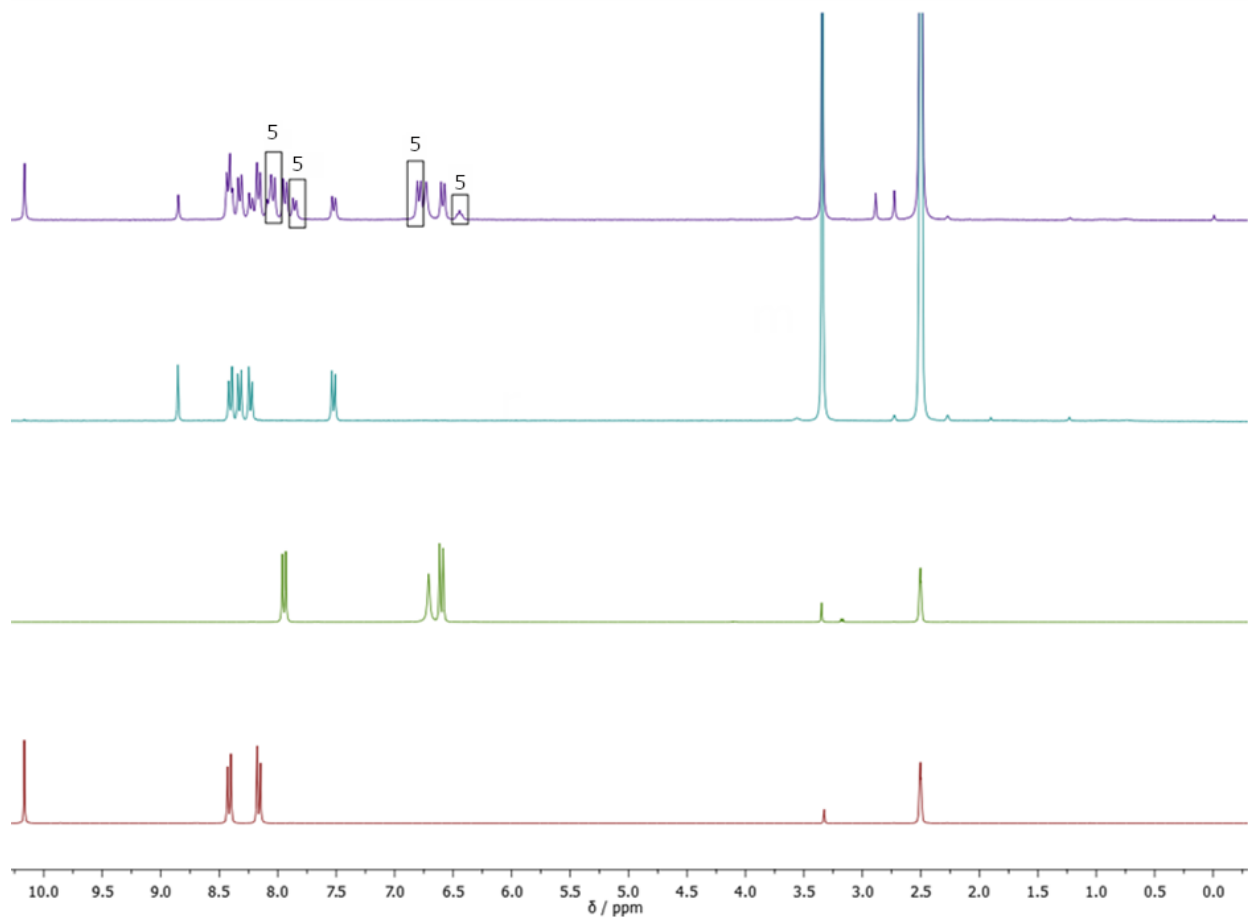


Figure S42. Comparison of ^1H NMR spectra (DMSO- d_6 , 300 MHz) previously depicted in Figure S41 with the spectra of starting materials **1** and **2**, and pure imine **3**. Marked signals belong to aminal.

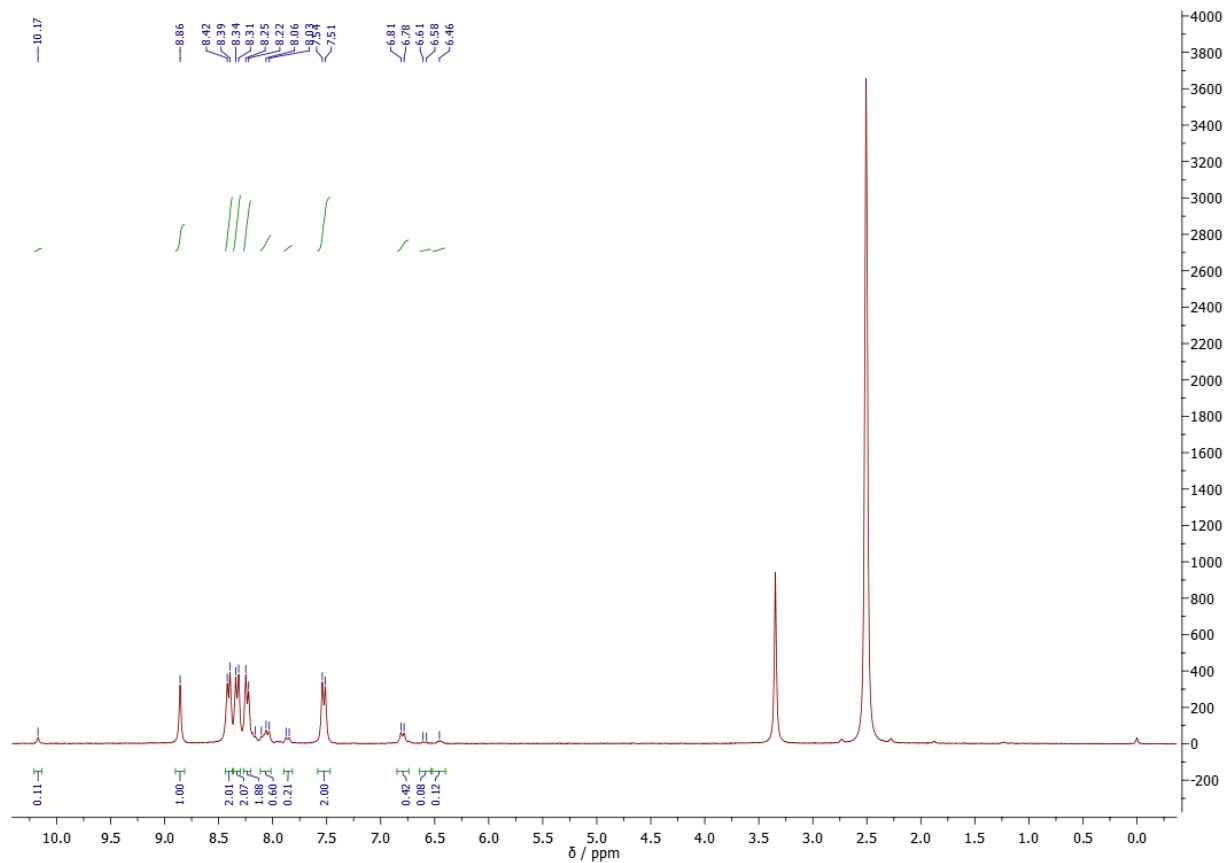


Figure S43. ^1H NMR spectrum of the reaction mixture obtained by grinding **1** and **2** with AcOH as a catalyst for 60 min (DMSO- d_6 , 300 MHz).

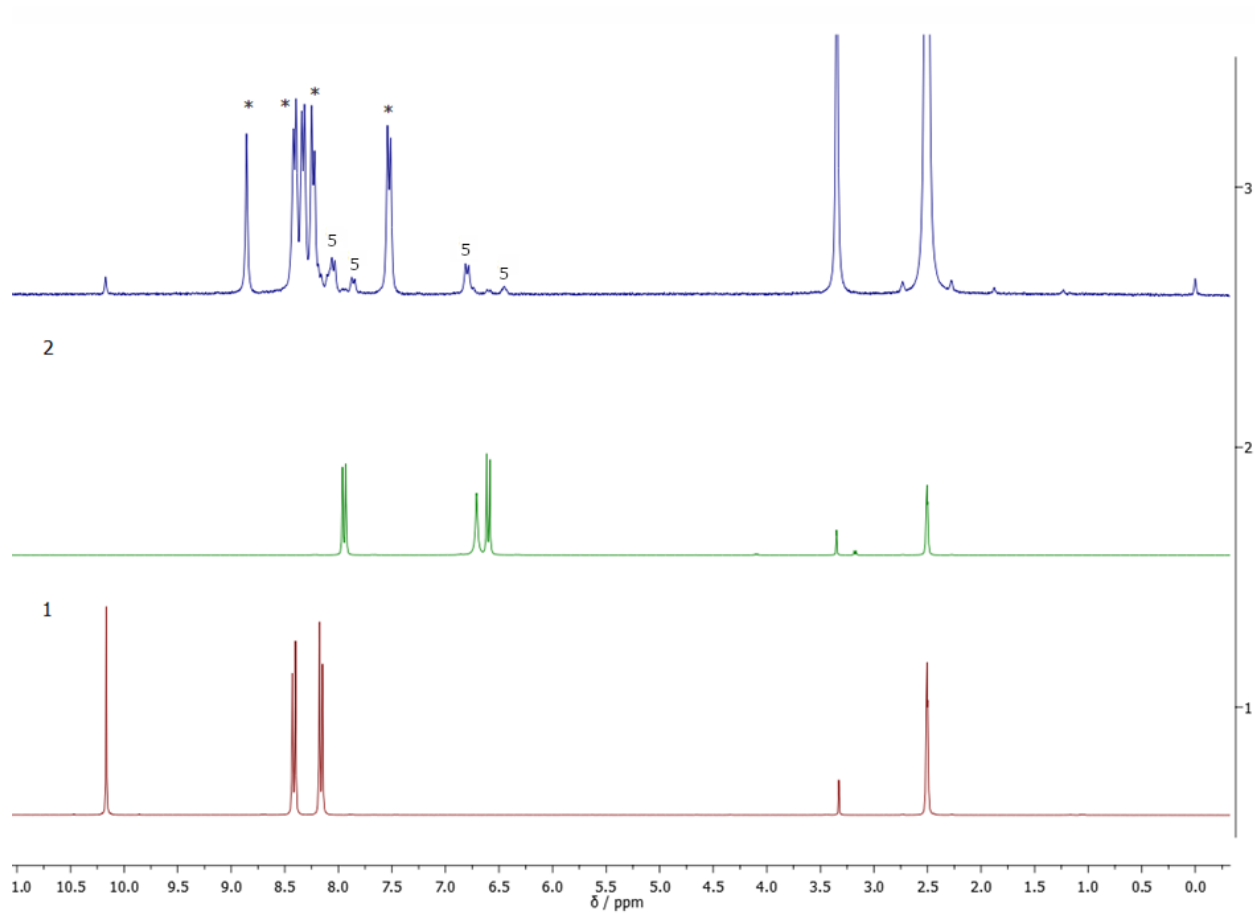


Figure S44. Comparison of ^1H NMR spectra (DMSO- d_6 , 300 MHz) of the reaction mixture after performing the reaction with AcOH for 60 min (top, blue line) with starting materials **1** and **2**. Marked signals belong to imine (*) and aminal.

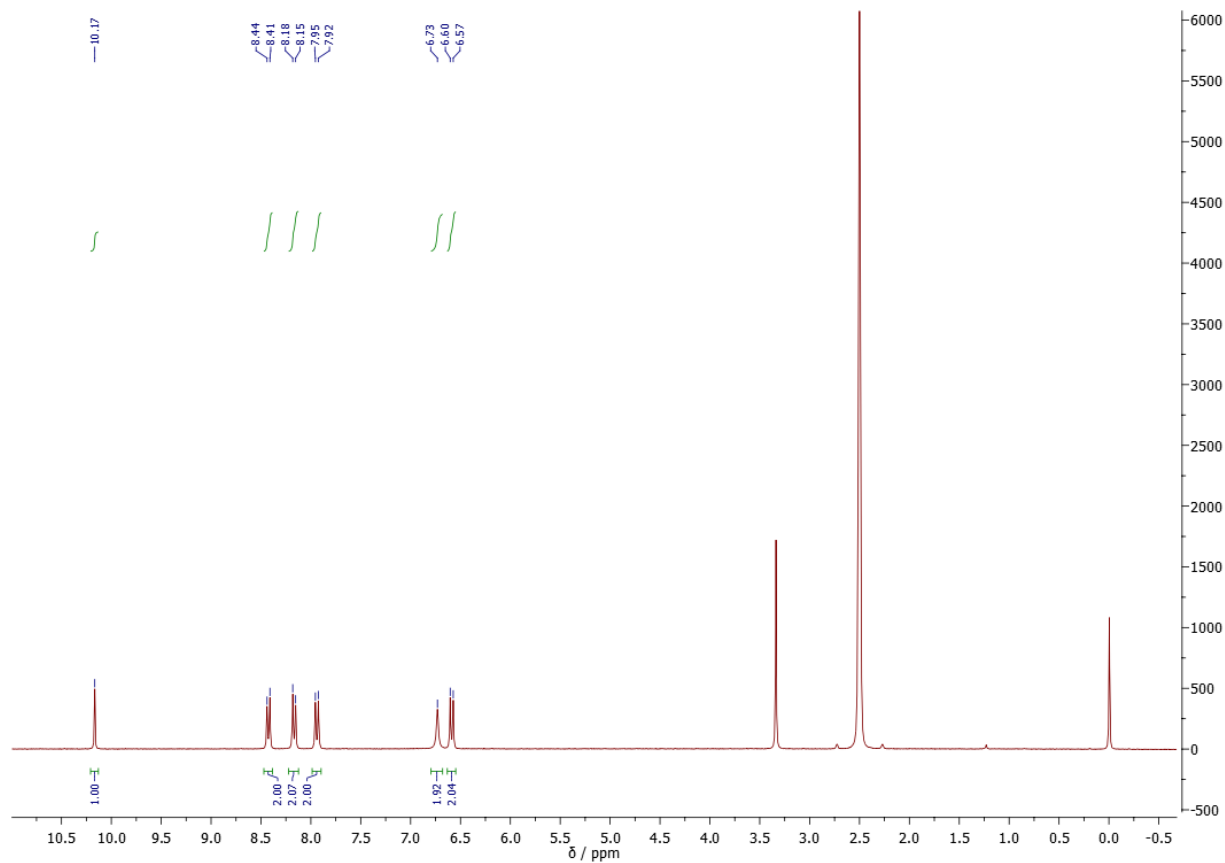


Figure S45. ^1H NMR spectrum of the reaction mixture obtained by grinding **1** and **2** with TEA as an additive for 60 min (DMSO- d_6 , 300 MHz).

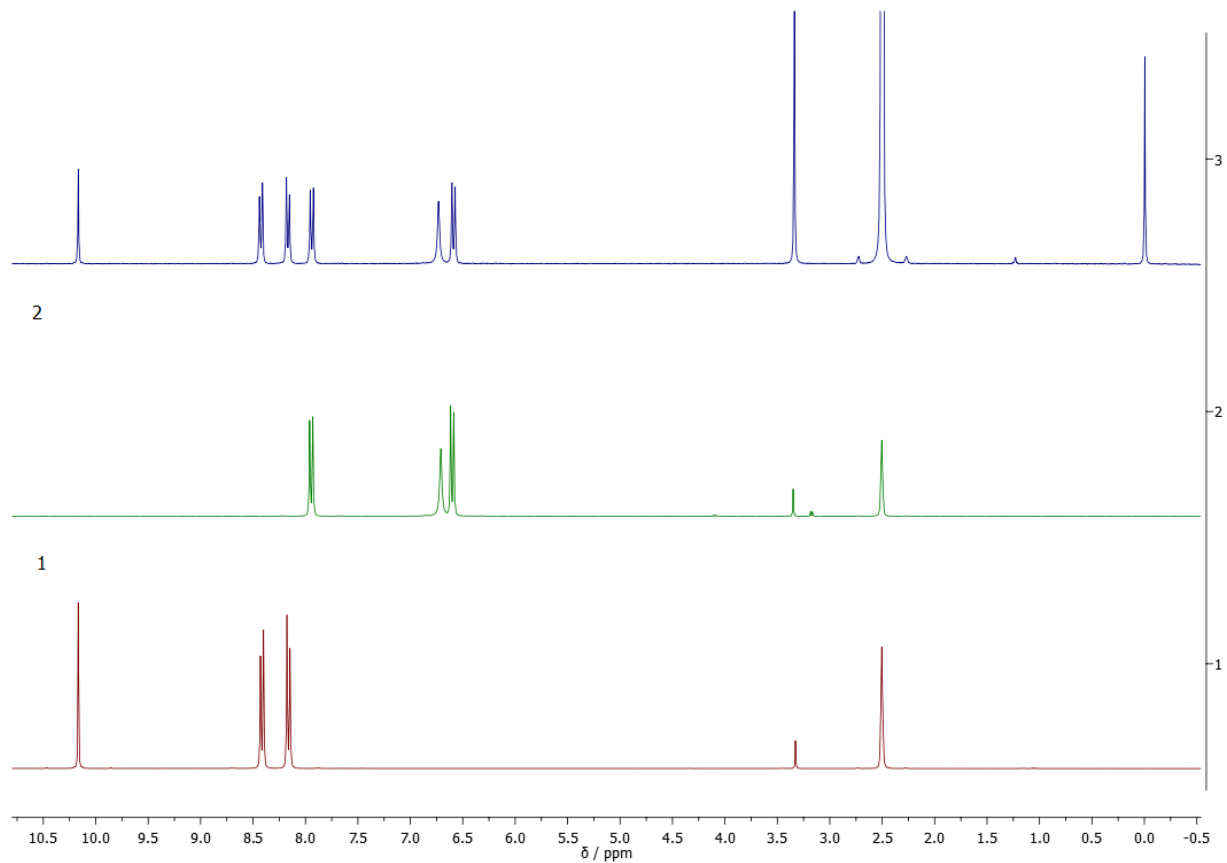


Figure S46. Comparison of ^1H NMR spectra (DMSO- d_6 , 300 MHz) of the reaction mixture after performing the reaction with TEA for 60 min (top, blue line) with starting materials **1** and **2**.

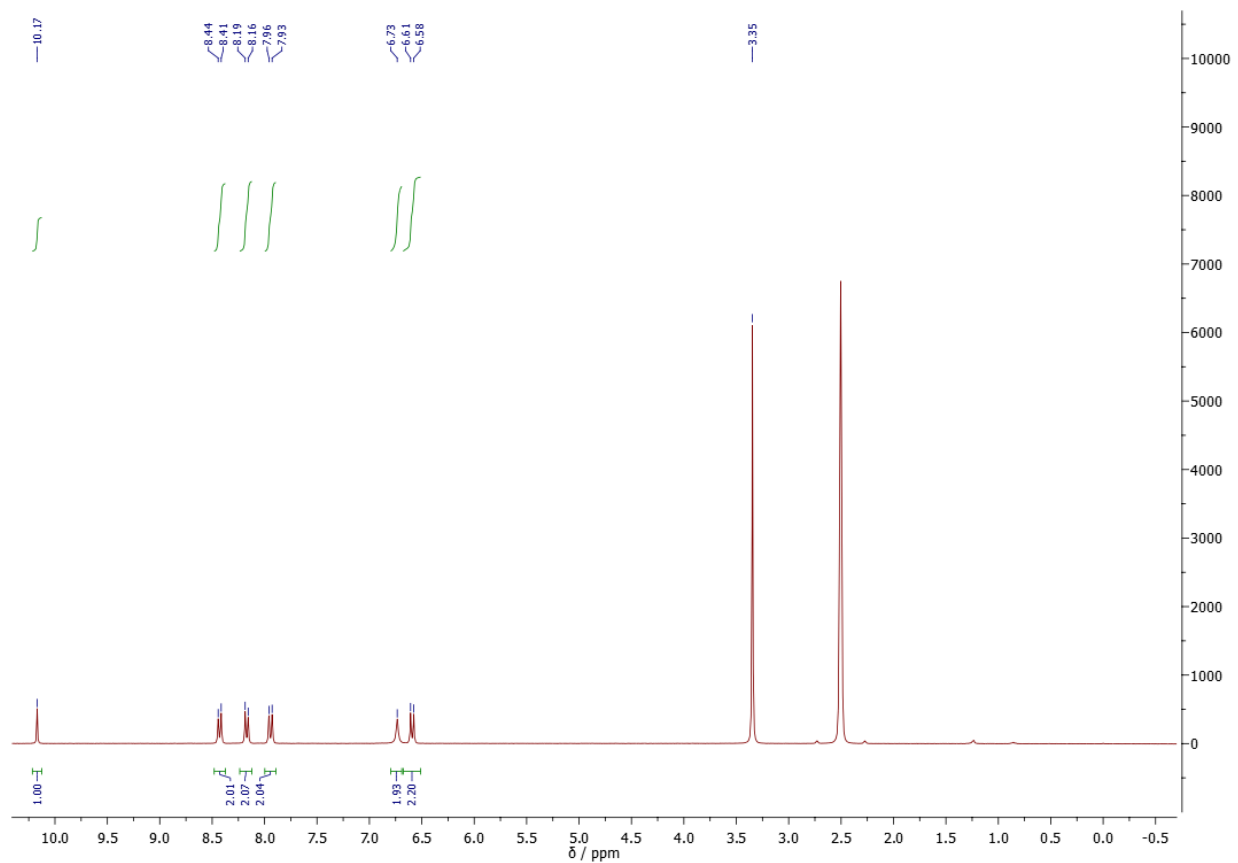


Figure S47. ^1H NMR spectrum (DMSO- d_6 , 300 MHz) of the reaction mixture obtained by grinding **1** and **2** with n-heptane for 60 min.

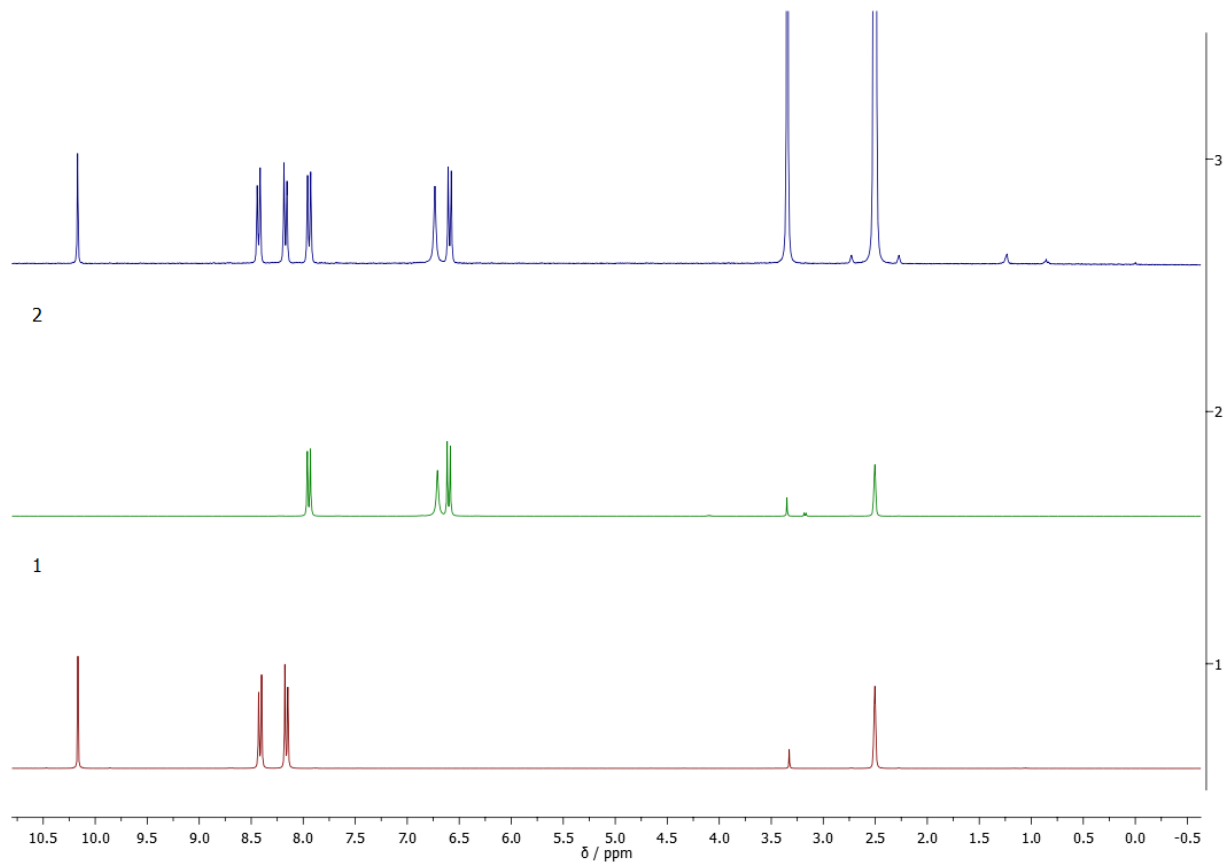


Figure S48. Comparison of ^1H NMR spectra (DMSO- d_6 , 300 MHz) of the reaction mixture after performing the reaction with n-heptane for 60 min (top, blue line) with starting materials **1** and **2**.

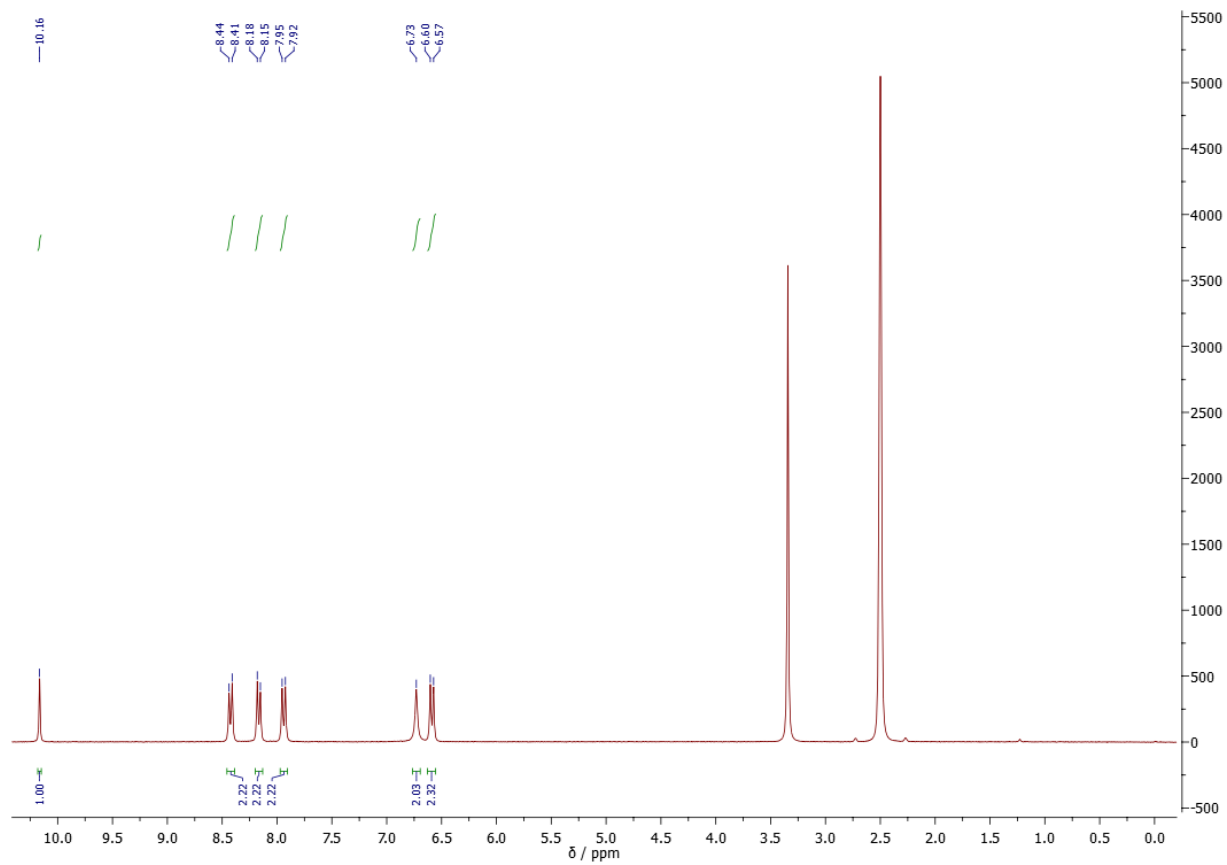


Figure S49. ^1H NMR spectrum (DMSO- d_6 , 300 MHz) of the reaction mixture obtained by grinding **1** and **2** with Et $_2$ O for 60 min.

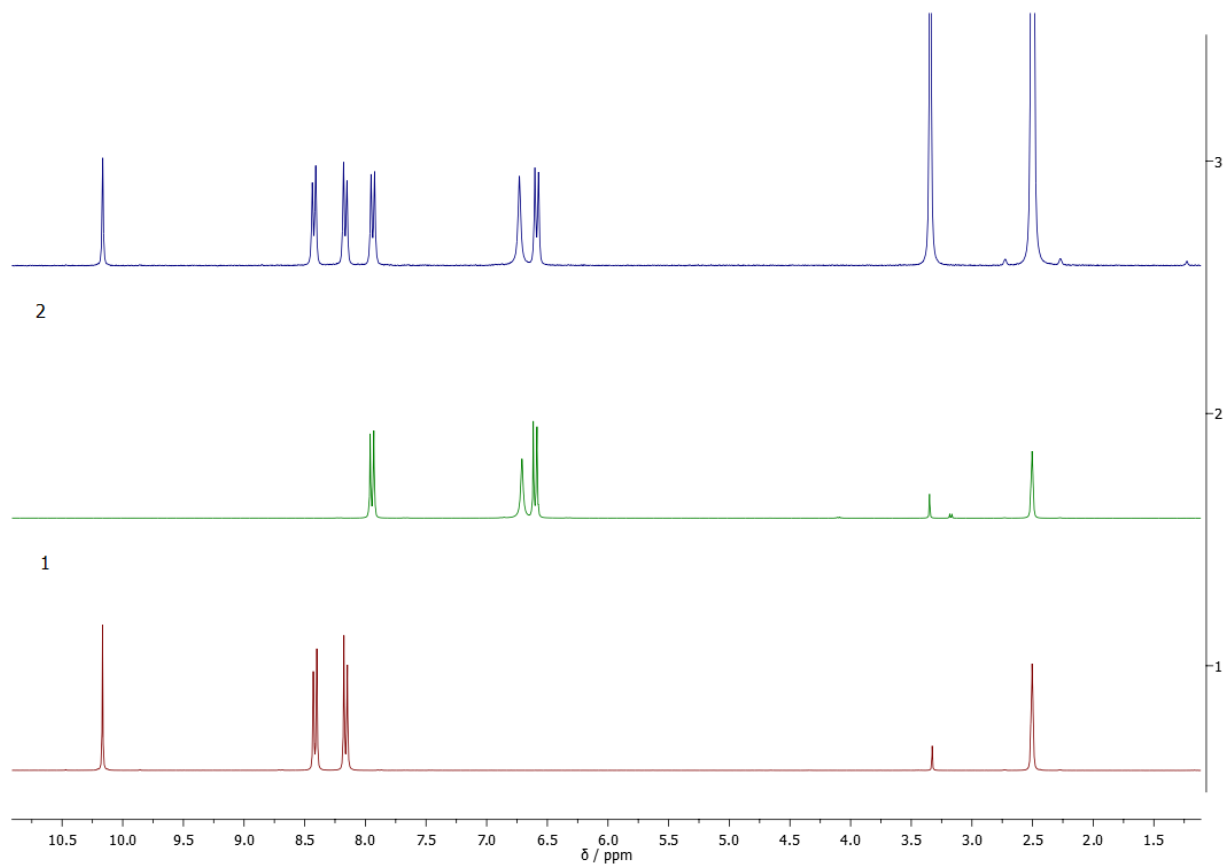


Figure S50. Comparison of ^1H NMR spectra (DMSO- d_6 , 300 MHz) of the reaction mixture after performing the reaction with Et_2O for 60 min (top, blue line) with starting materials **1** and **2**.

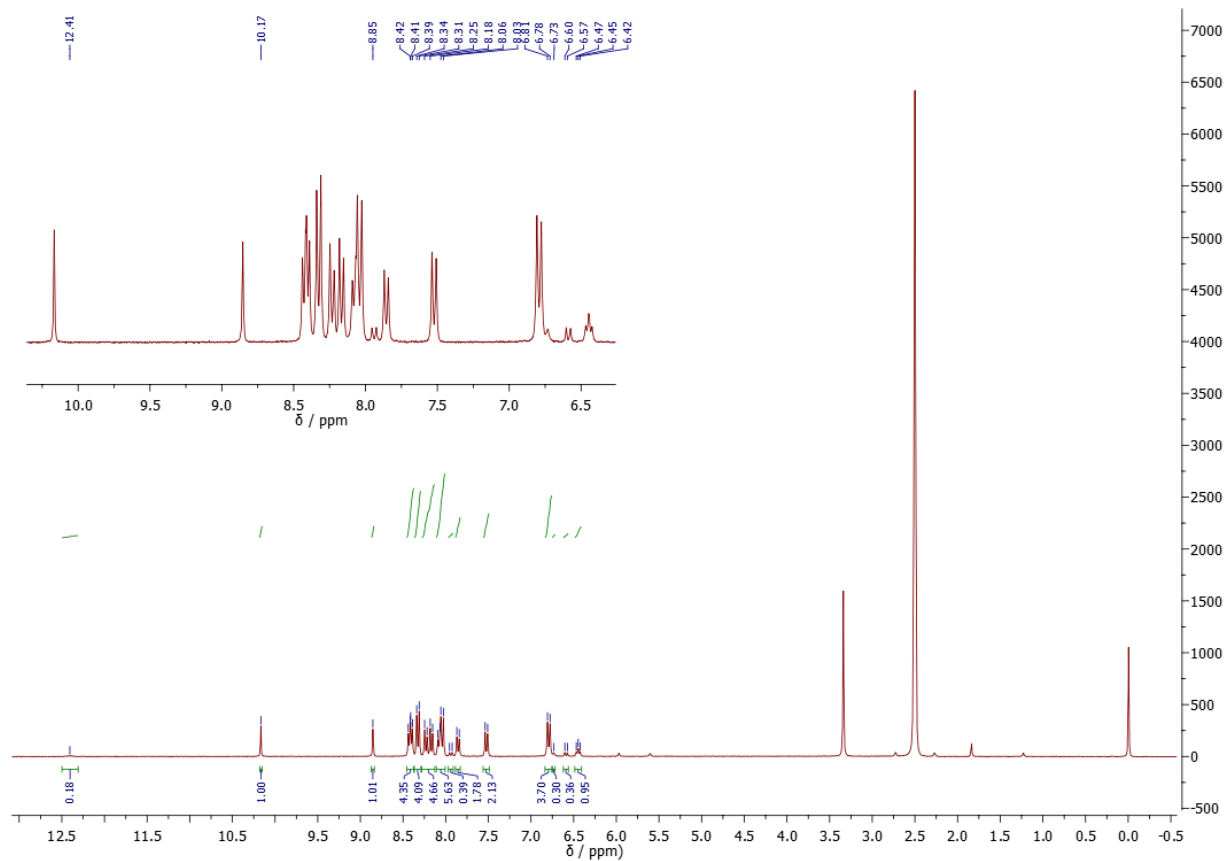


Figure S51. ^1H NMR spectrum of the reaction mixture obtained by grinding **1** and **2** with META as a catalyst for 60 min (DMSO- d_6 , 300 MHz).

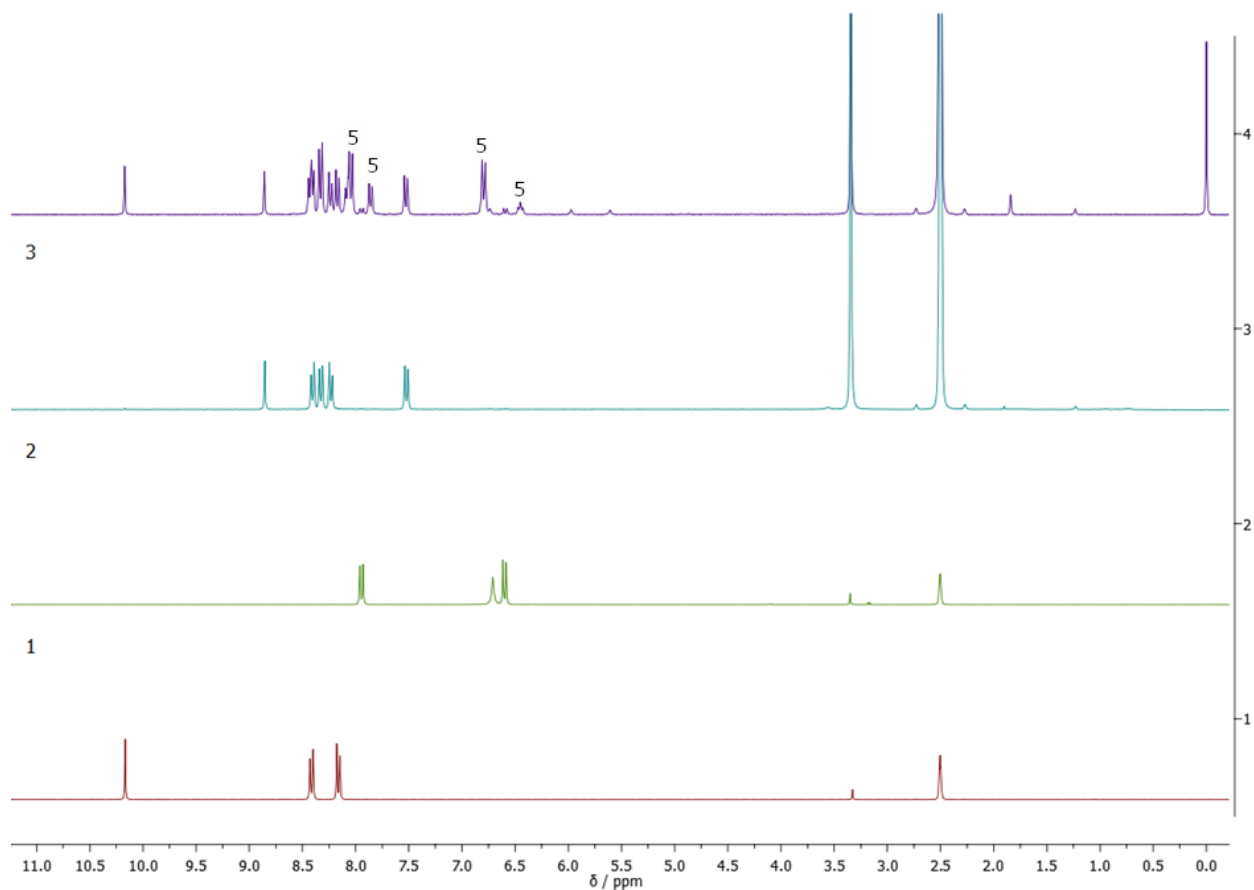


Figure S52. Comparison of ¹H NMR spectra (DMSO-*d*₆, 300 MHz) of the reaction mixture after performing the reaction with META for 60 min (top, purple line) with starting materials **1**, **2** and pure imine **3**. Marked signals belong to aminoral.

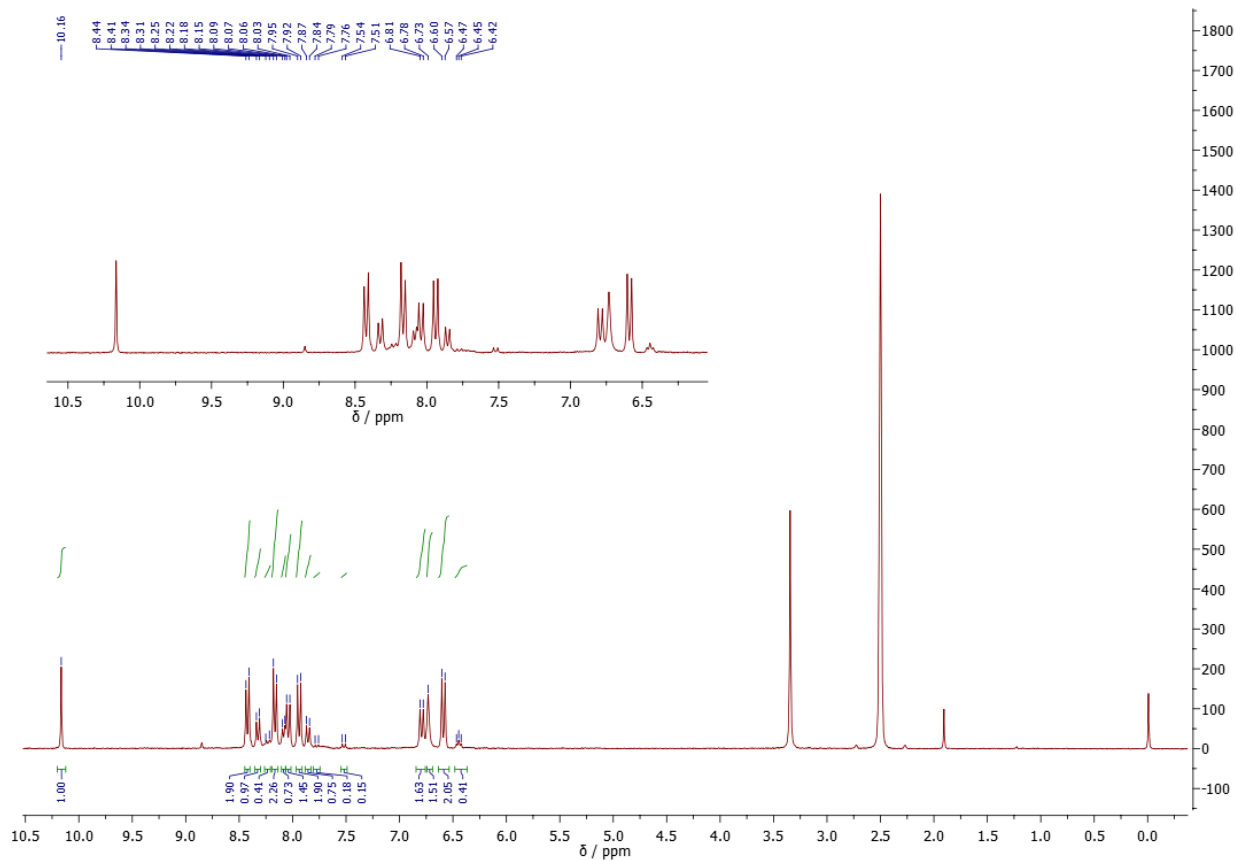


Figure S53. ^1H NMR spectrum of the reaction mixture obtained by grinding **1** and **2** with AMC as a catalyst for 60 min (DMSO- d_6 , 300 MHz).

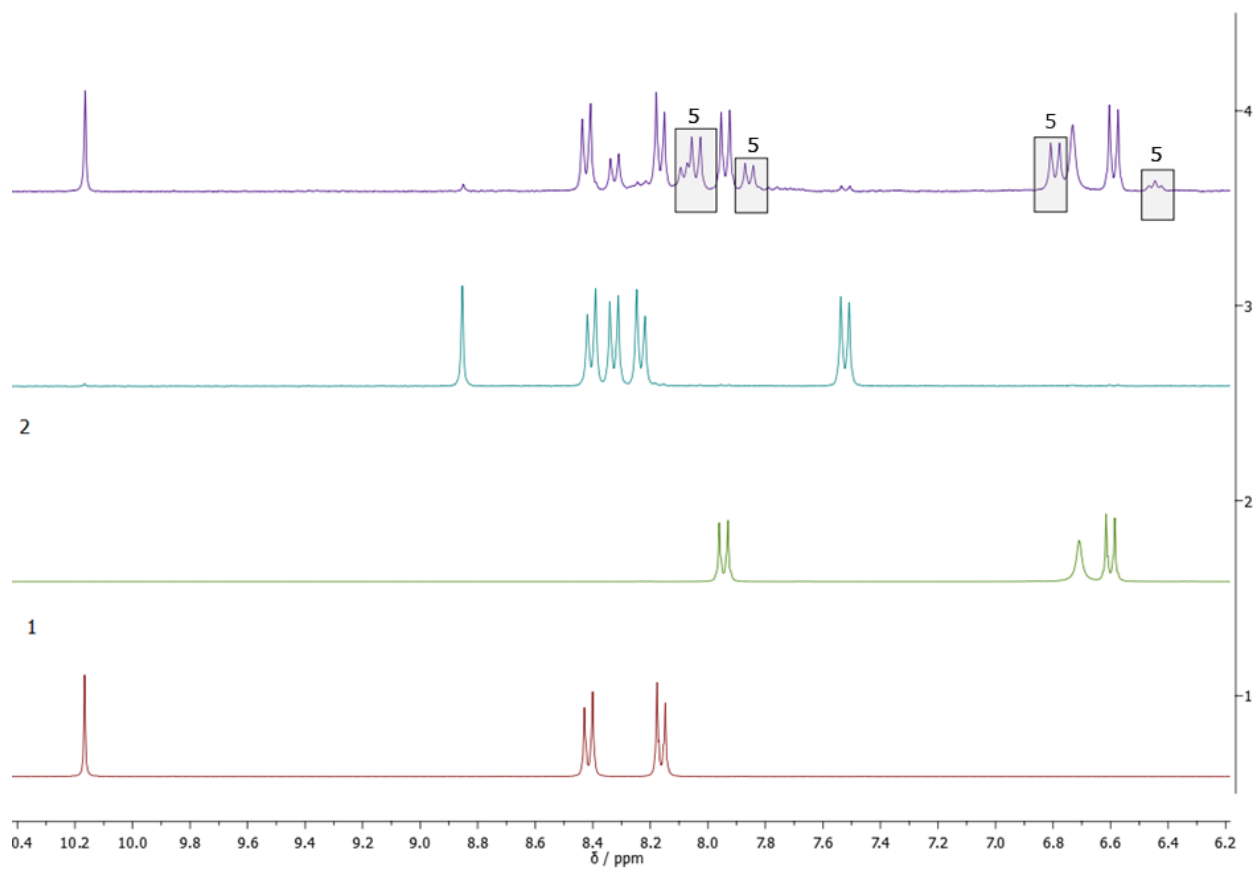


Figure S54. Comparison of ¹H NMR spectra (DMSO-*d*₆, 300 MHz) of the reaction mixture after performing the reaction with AMC for 60 min (top, purple line) with starting materials **1**, **2** and pure imine **3**. Marked signals belong to aminal.

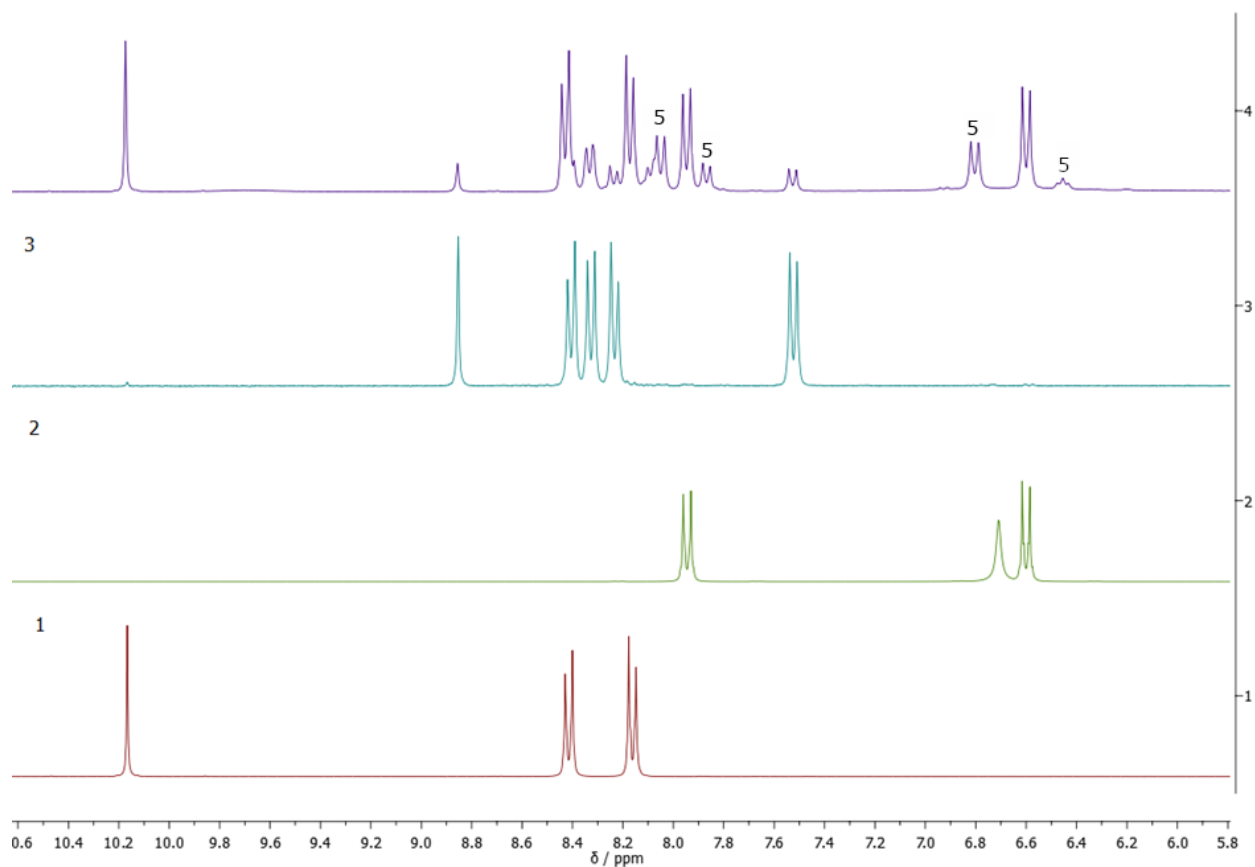


Figure S56. Comparison of ¹H NMR spectra (DMSO-*d*₆, 300 MHz) of the reaction mixture after performing the reaction with SA during 60 min (top, purple line) with starting materials **1**, **2** and pure imine **3**. Marked signals belong to aminoral.

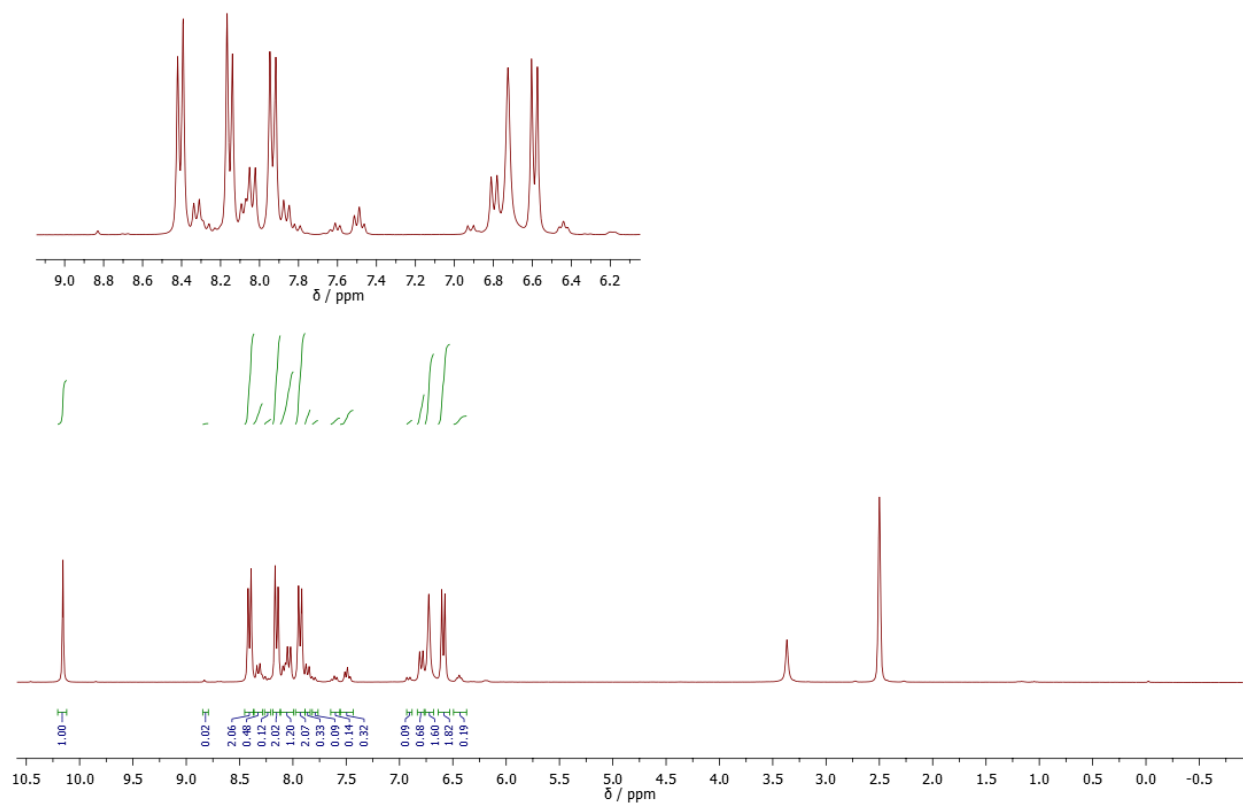


Figure S57. ^1H NMR spectrum of the reaction mixture obtained by grinding **1** and **2** with BA as a catalyst during 60 min ($\text{DMSO-}d_6$, 300 MHz). The same signals for a mineral were observed.

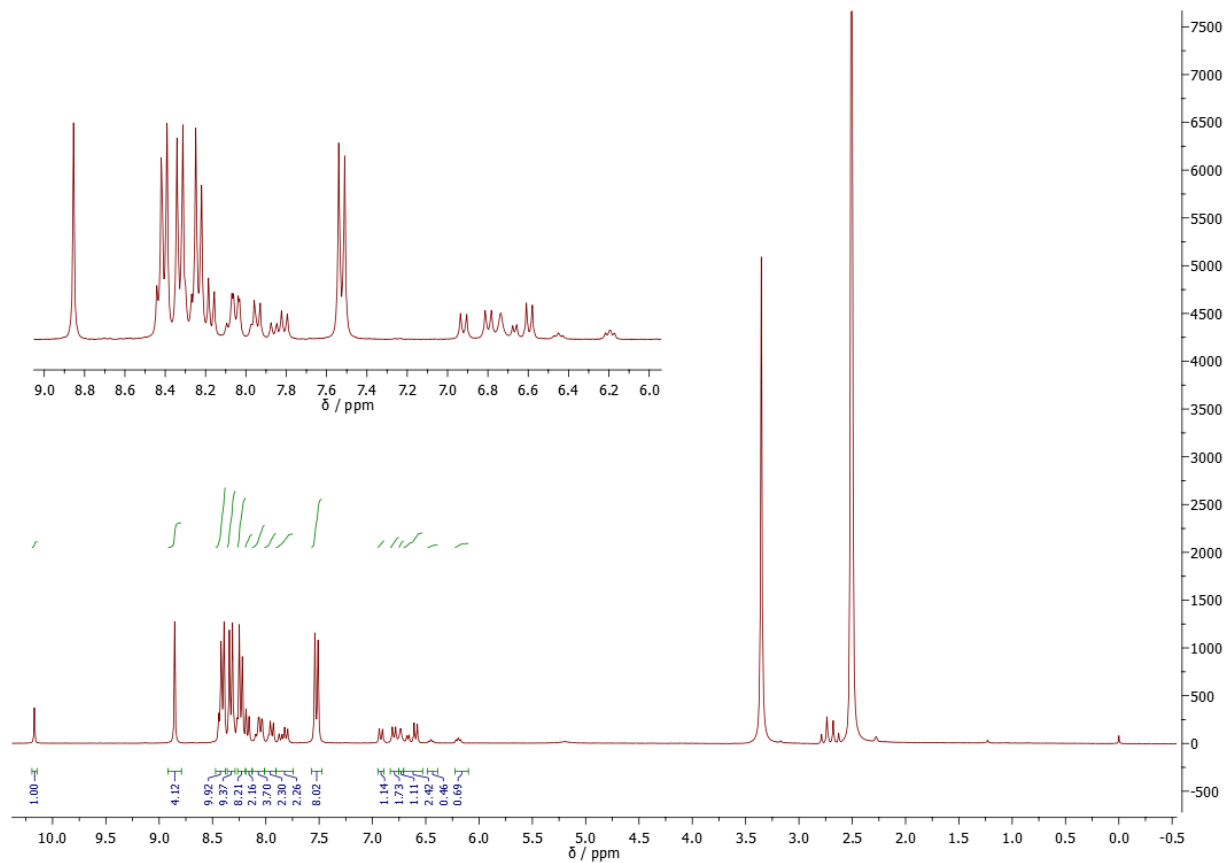


Figure S58. ^1H NMR spectrum of the reaction mixture obtained by grinding **1** and **2** with CA as a catalyst for 60 min ($\text{DMSO}-d_6$, 300 MHz). The same signals for aminal were observed.

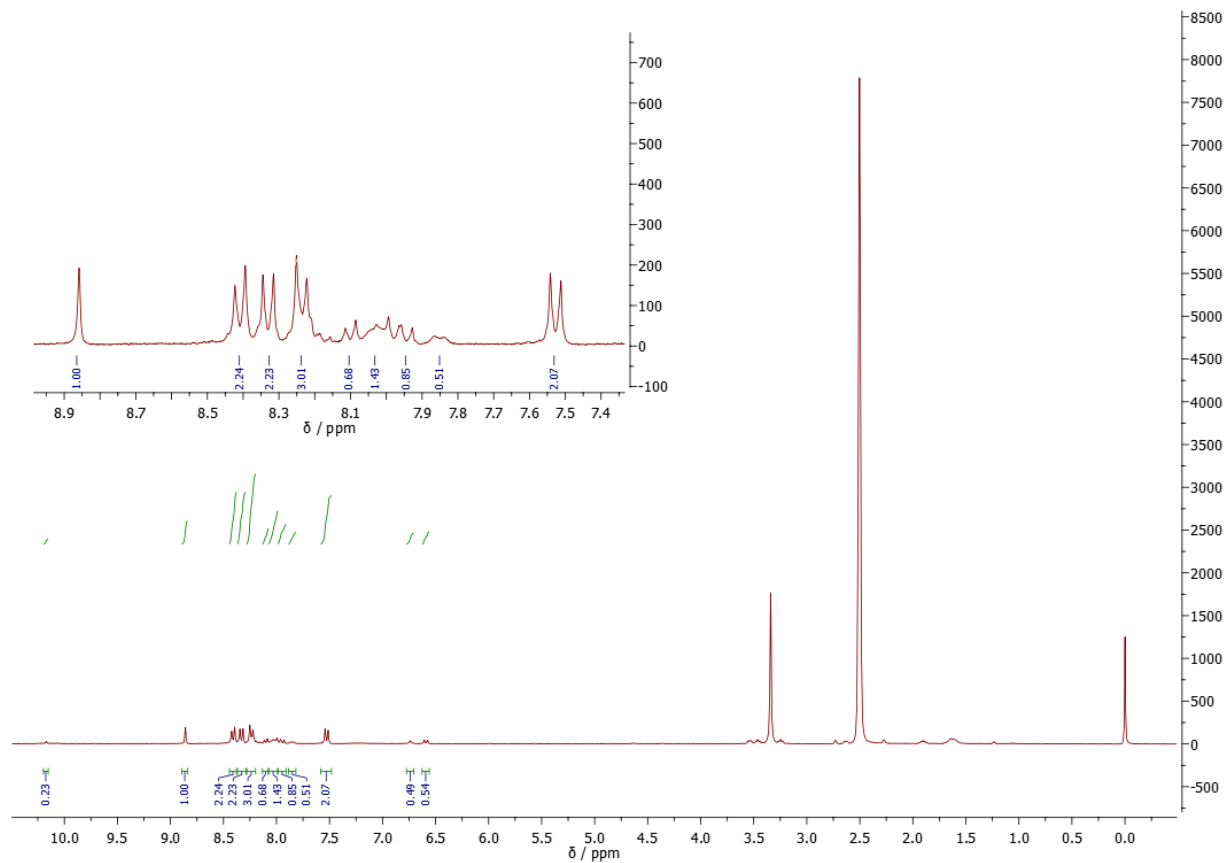


Figure S59. ^1H NMR spectrum of the reaction mixture obtained by grinding **1** and **2** with DBU as a catalyst for 60 min ($\text{DMSO-}d_6$, 300 MHz). The same signals for a mineral were observed.

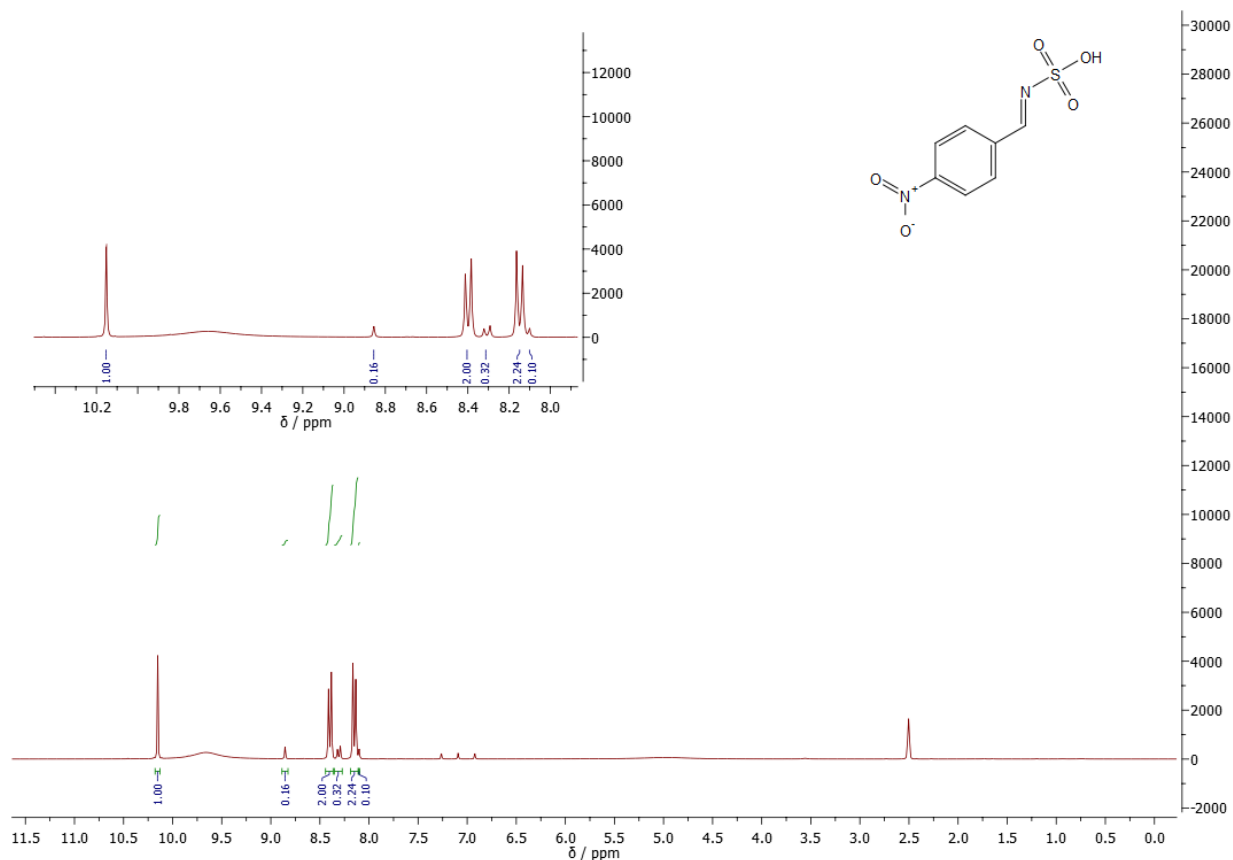


Figure S60. ^1H NMR spectrum of the reaction mixture obtained by grinding **1** and SA in molar ratio 1:1 for 60 min ($\text{DMSO}-d_6$, 300 MHz).

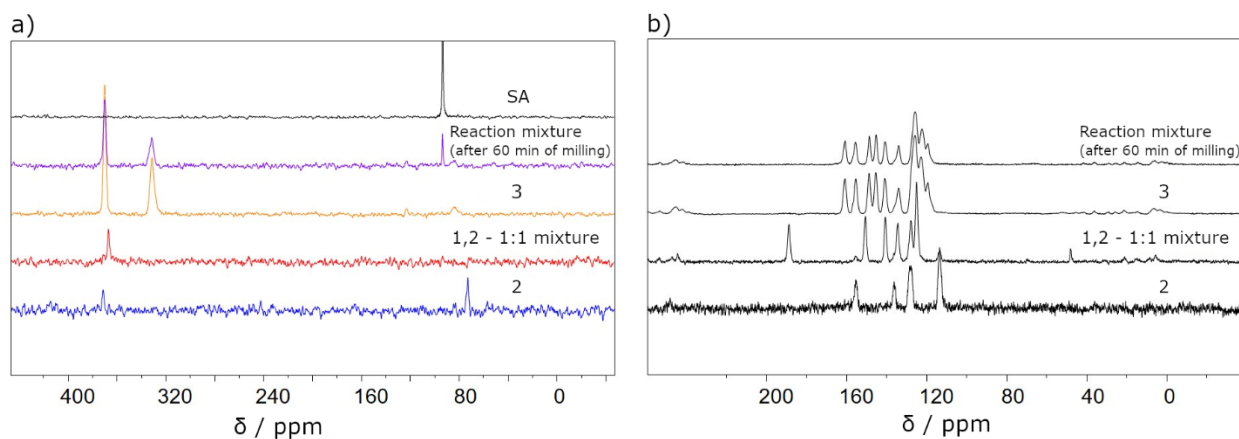


Figure S61. a) ^{15}N and b) ^{13}C CP-MAS solid-state NMR spectra of the starting materials **1** and **2**, the isolated imine **3** and the reaction mixture using SA in a catalytic amount (0.1 eq).

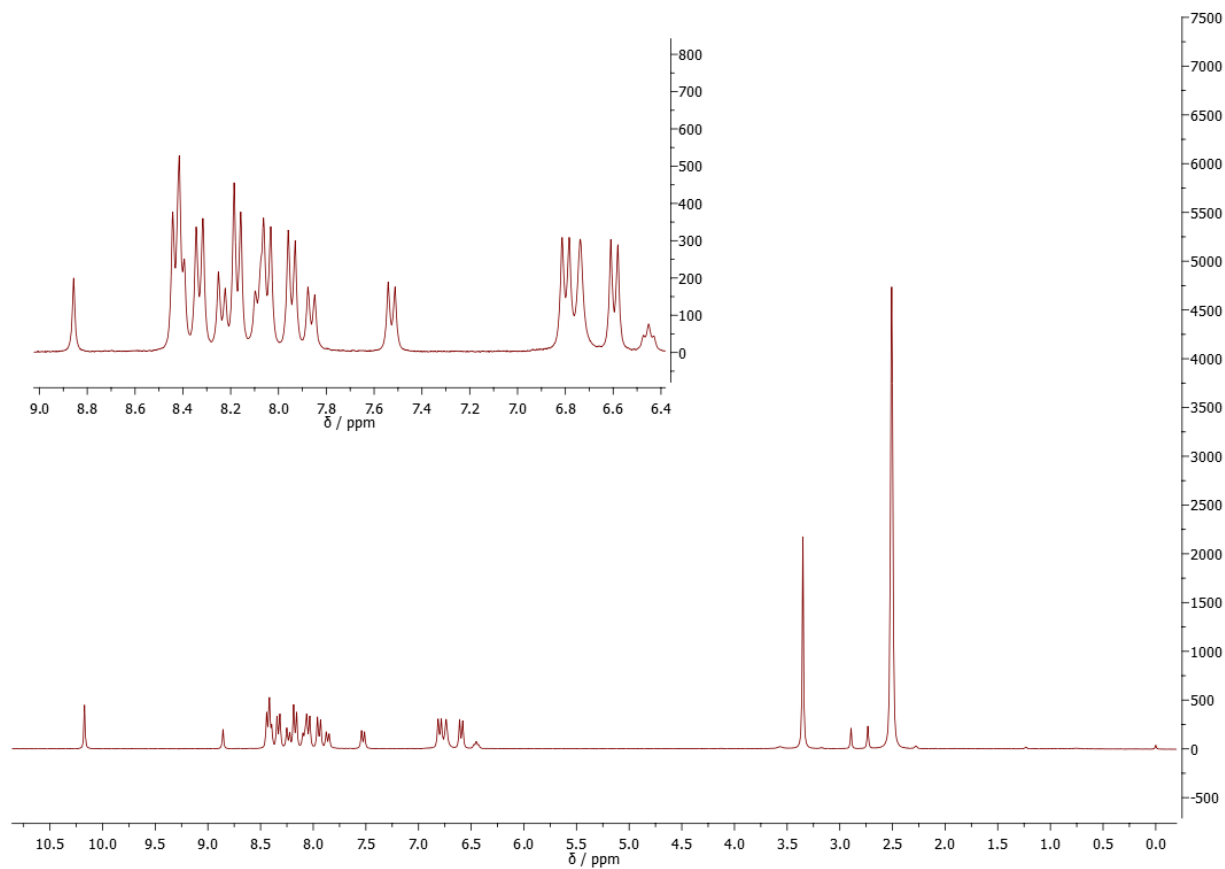


Figure S62. a) 1D ^1H NMR spectrum of the reaction mixture obtained by grinding **1** and **2** with DMF after 60 min of grinding ($\text{DMSO-}d_6$, 600 MHz). The same reaction mixture was further sent for 2D ^1H - ^1H COSY analysis.

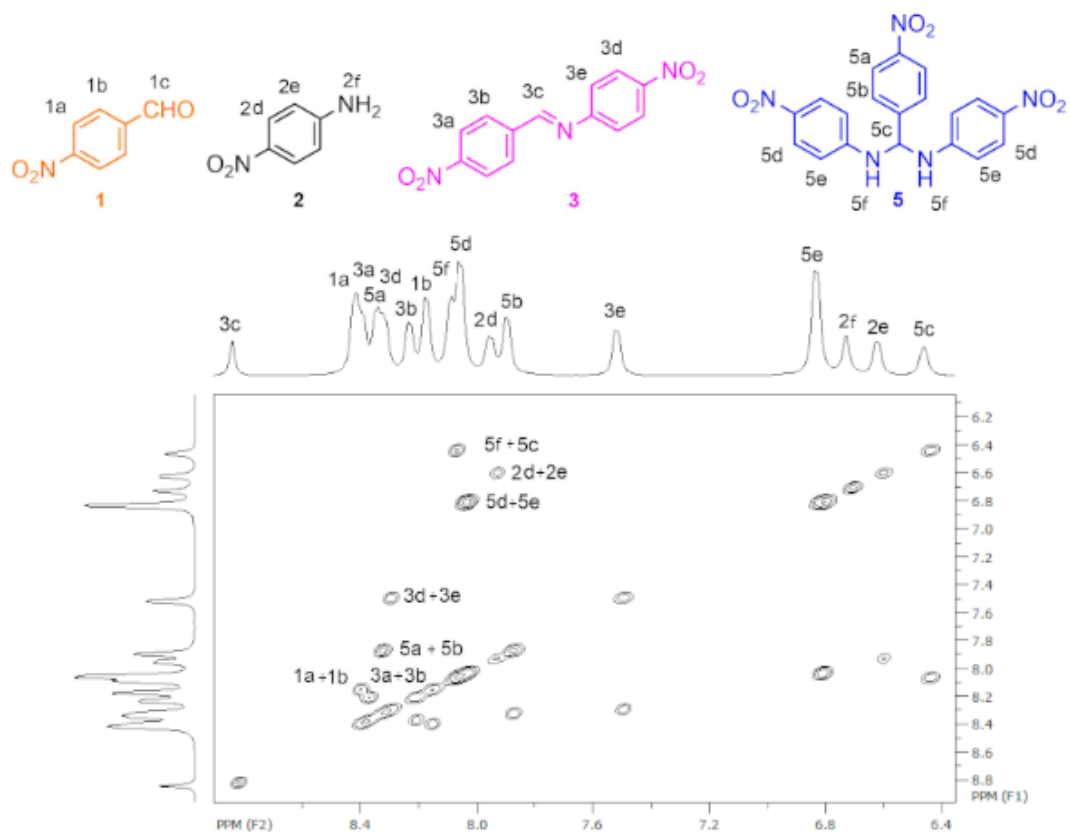


Figure S62. b) 2D ¹H-¹H COSY spectrum of the reaction mixture obtained by grinding **1** and **2** with DMF after 60 min of grinding (DMSO-*d*₆, 600 MHz).

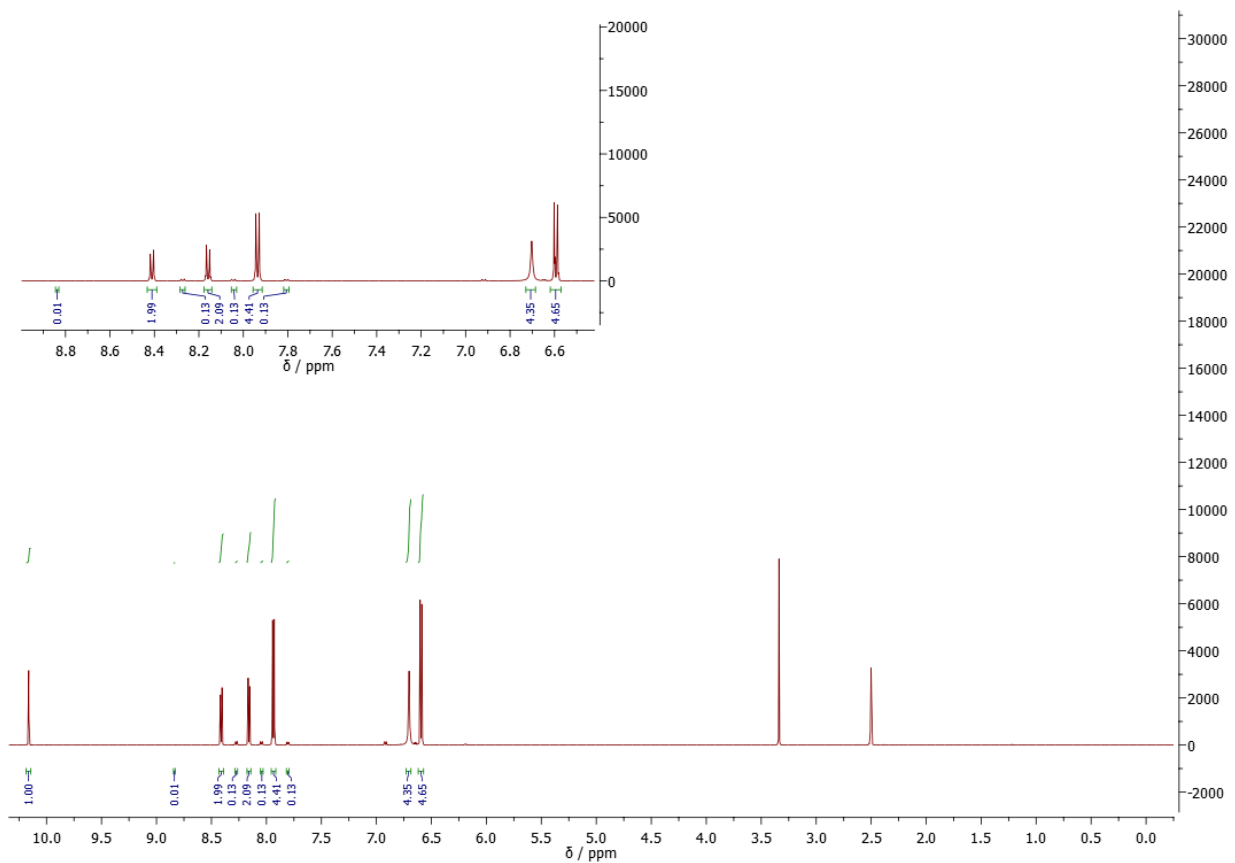


Figure S63. ^1H NMR spectrum (DMSO- d_6 , 300 MHz) of the reaction mixture obtained by grinding **1** and **2** in a molar ratio 1:2 for 60 min.

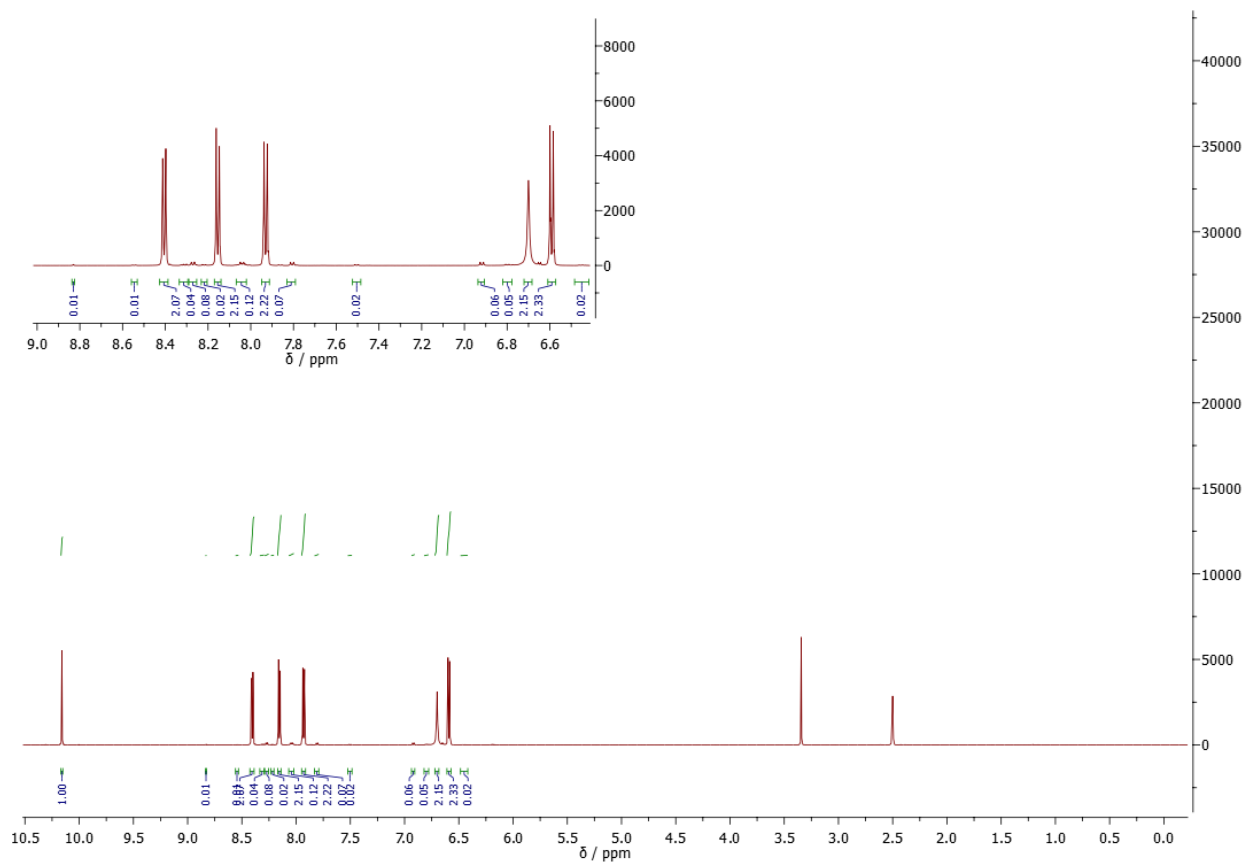


Figure S64. ^1H NMR spectrum (DMSO- d_6 , 300 MHz) of the reaction mixture obtained by grinding **1** and **2** in a molar ratio 1:2 for 240 min.

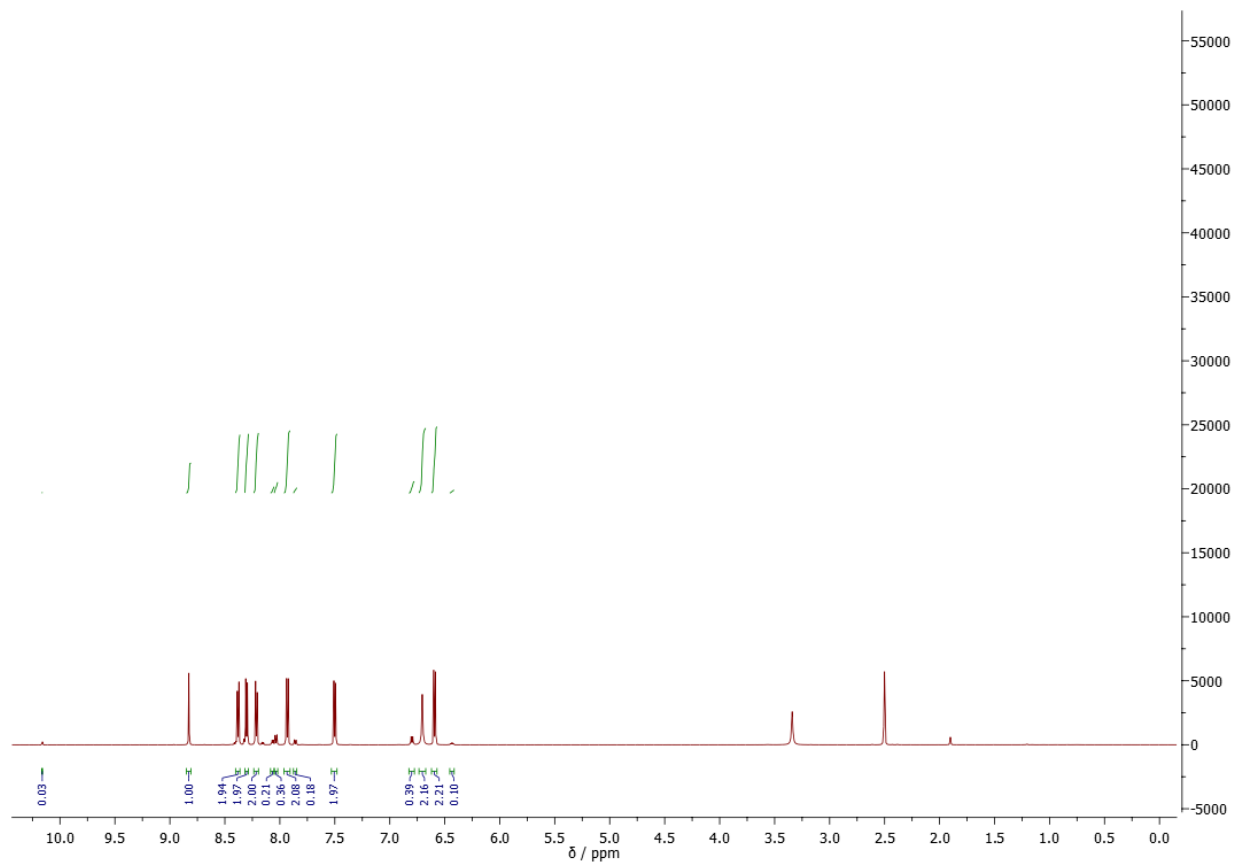


Figure S65. a) ^1H NMR spectrum (DMSO- d_6 , 300 MHz) of the reaction mixture obtained by grinding **1** and **2** in a molar ratio 1:2 with acetic acid (0.1 equiv.) for 240 min.

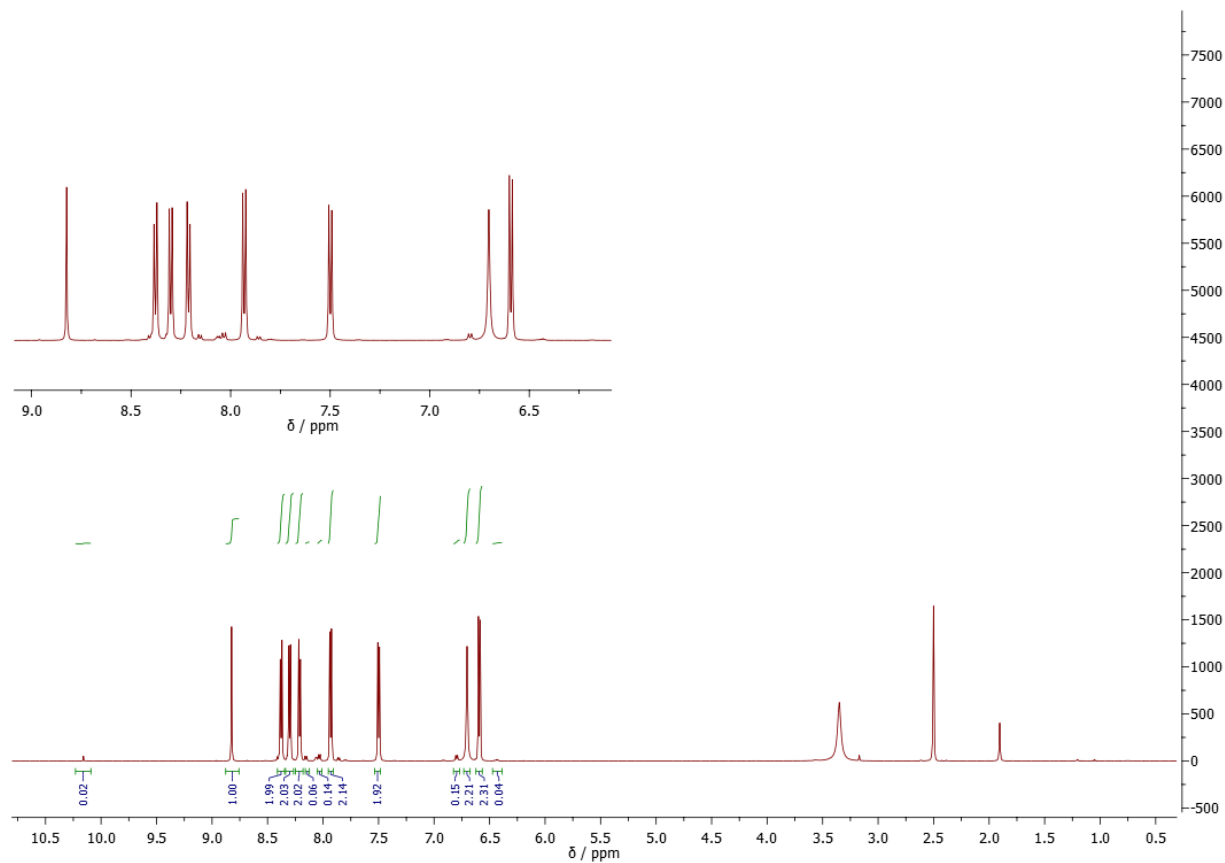


Figure S66. b) ^1H NMR spectrum (DMSO- d_6 , 300 MHz) of the reaction mixture obtained by grinding **1** and **2** in a molar ratio 1:2 with acetic acid (0.1 equiv.) for 120 min. The same experiment was conducted for shorter milling time (120 min) in order to trap an aminor.

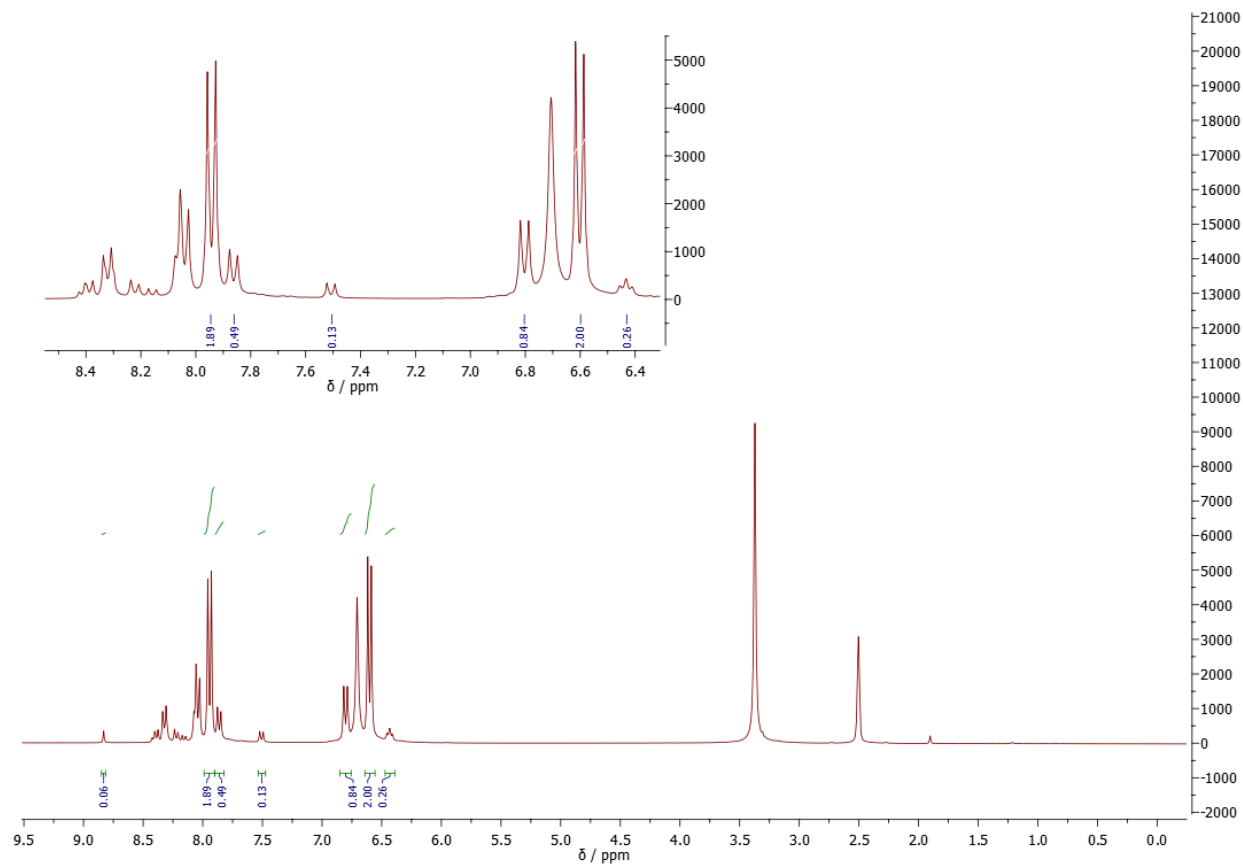


Figure S67. ^1H NMR spectrum ($\text{DMSO-}d_6$, 300 MHz) of the reaction mixture obtained by grinding **1** and **2** in a molar ratio 1:5 with acetic acid (0.1 equiv.) after 120 min. The aminal **5** was formed in 19% yield (6.45 ppm) and imine in 4% yield (8.85 ppm). The yield was calculated according to the peak integrals of the desired compound and the starting material.

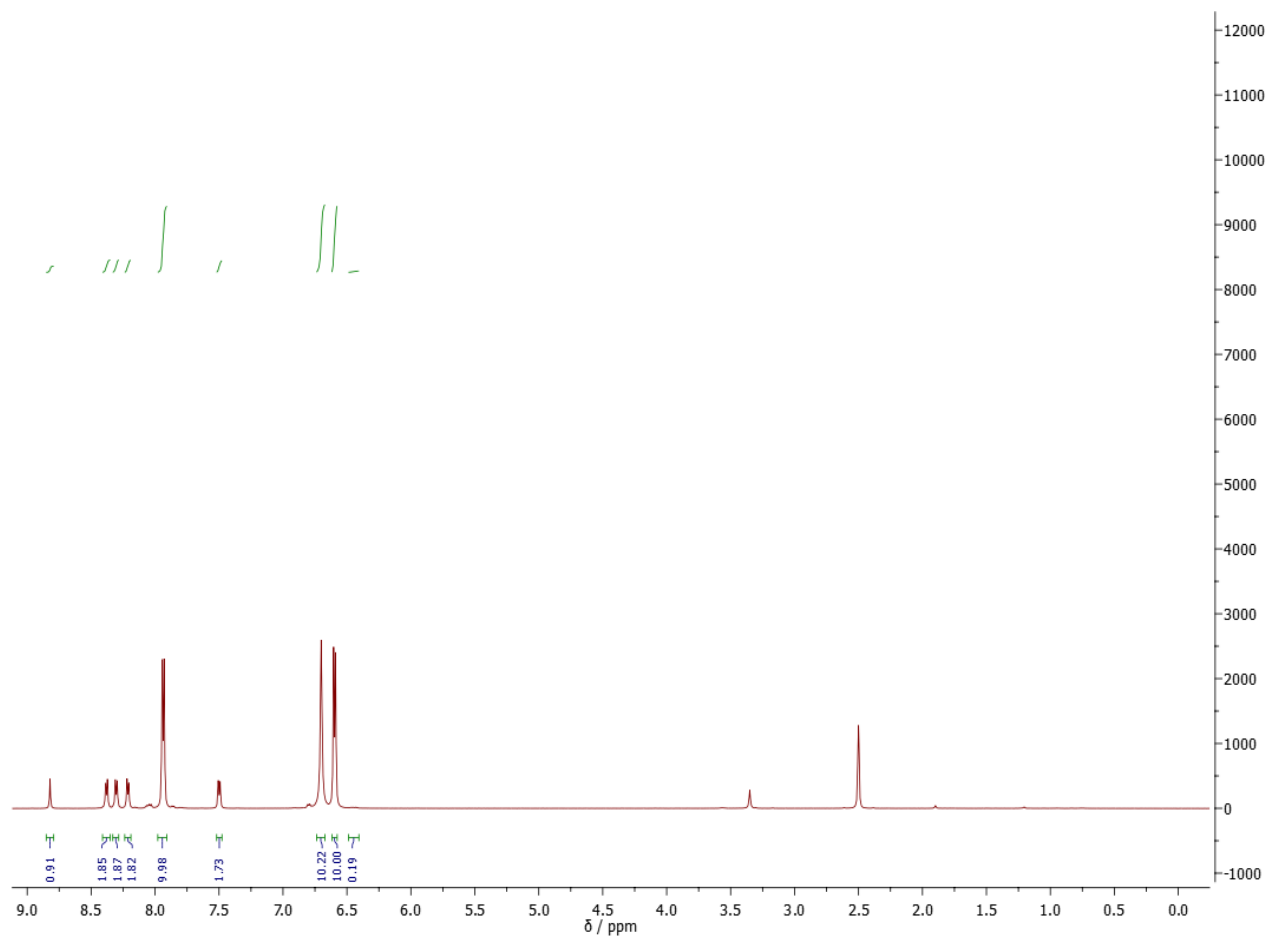


Figure S68. ^1H NMR spectrum ($\text{DMSO-}d_6$, 300 MHz) of the reaction mixture obtained by grinding **3** and **2** in a molar ratio 1:5 with acetic acid (0.1 equiv.) for 60 min.

Table S2. NMR percentage of compounds **3** and **5** in observed ^1H NMR spectra after 60 min of grinding the equimolar quantities of starting materials, unless otherwise noted (calculated by moles of present species in the mixture). Entries 8 and 9 provide evidence for the formation of **5** from the hemiaminal and not from the imine.

		Product 3	Product 5
	# of H's in peak	1.00	1.00
	Chemical shift (ppm)	8.85	6.45
	MW (g/mol)	271.23	409.36
	Additive (ratio, time)	(% by moles)	
1	MeCN	0.9	2.4
2	DMF ^a	17	18
3	DMF ^b	13	30
4	DMF ^c	50	1
5	AcOH	81	8
6	AcOH ^d	45	4
7	AcOH ^e	49	1.8
8	AcOH^f	5	20
9	AcOH^g	14	3
10	META	32	30
11	DBU	51	13
12	AMC	5	15
13	SA	10	16
14	SA ^h	5	12
15	BA	1	6
16	CA	65	7
17	Neat ⁱ	0.5	7.4

^aAnalysis of reaction mixture sampled after 60 min of grinding and aged for several days. ^bReaction mixture sampled after overnight grinding, the contamination with stainless steel ball broad NMR signals. ^cMilling of **2** and **3** in a molar ratio 1:1 with 0.1 equiv. of DMF (without DMF, yield of **3** is 47% and **5** is 4%). ^dMilling of **1** and **2** in a molar ratio 1:2 with 0.1 equiv. of AcOH for 240 min. ^eMilling of **1** and **2** in a molar ratio 1:2 with 0.1 equiv. of AcOH after 120 min. ^fMilling of **1** and **2** in a molar ratio 1:5 with 0.1 equiv. of AcOH for 240 min. ^gMilling of **2** and **3** in a molar ratio 5:1 with 0.1 equiv. of AcOH for 240 min. ^hMilling of **1** and **2** in a molar ratio 1:2 with 0.1 equiv. of SA for 240 min. ⁱNeat milling of **1** and **2** in a molar ratio 1:2.

3.0. References

- (1) S. Lukin, K. Užarević, I. Halasz, Raman Spectroscopy for Real-Time and in Situ Monitoring of Mechanochemical Milling Reactions. *Nat. Protoc.* **2021**, *16*, 3492–3521.
- (2) Gaussian 16, Revision C.01, M. J. Frisch, G. W. Trucks, H. B. Schlegel, G. E. Scuseria, M. A. Robb, J. R. Cheeseman, G. Scalmani, V. Barone, G. A. Petersson, H. Nakatsuji, X. Li, M. Caricato, A. V. Marenich, J. Bloino, B. G. Janesko, R. Gomperts, B. Mennucci, H. P. Hratchian, J. V. Ortiz, A. F. Izmaylov, J. L. Sonnenberg, D. Williams-Young, F. Ding, F. Lipparini, F. Egidi, J. Goings, B. Peng,

A. Petrone, T. Henderson, D. Ranasinghe, V. G. Zakrzewski, J. Gao, N. Rega, G. Zheng, W. Liang, M. Hada, M. Ehara, K. Toyota, R. Fukuda, J. Hasegawa, M. Ishida, T. Nakajima, Y. Honda, O. Kitao, H. Nakai, T. Vreven, K. Throssell, J. A. Montgomery, Jr., J. E. Peralta, F. Ogliaro, M. J. Bearpark, J. J. Heyd, E. N. Brothers, K. N. Kudin, V. N. Staroverov, T. A. Keith, R. Kobayashi, J. Normand, K. Raghavachari, A. P. Rendell, J. C. Burant, S. S. Iyengar, J. Tomasi, M. Cossi, J. M. Millam, M. Klene, C. Adamo, R. Cammi, J. W. Ochterski, R. L. Martin, K. Morokuma, O. Farkas, J. B. Foresman, and D. J. Fox, Gaussian, Inc., Wallingford CT, 2016.

- (3) C.-W. Chen, M.-C. Tseng, S.-K. Hsiao, W.-H. Chen, Y.-H. Chu, Transimination Reactions in [b-3C-Im][NTf₂] Ionic Liquid. *Org. Biomol. Chem.* **2011**, *9*, 4188.
- (4) H. B. Bürgi, J. D. Dunitz, C. Züst, Lattice Parameters and Space Groups of Some Aromatic Schiff Bases. *Acta Crystallogr. B Struct. Sci.* **1968**, *24*, 463–464.